

CR-134053

17618-H090-R0-00

PROJECT TECHNICAL REPORT

APOLLO CRYOGENIC SYSTEMS PROGRAMS

MSC/TRW TASK 705-2

NAS 9-8166

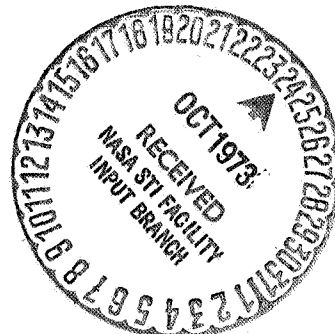
DECEMBER, 1970

Prepared for
NATIONAL AERONAUTICS AND SPACE ADMINISTRATION
MANNED SPACECRAFT CENTER
HOUSTON, TEXAS

(NASA-CR-134053) APOLLO CRYOGENIC SYSTEMS
PROGRAMS (TRW Systems Group) 99 p

N73-74104

00/99 Unclass
18664



TRW
SYSTEMS GROUP

PROJECT TECHNICAL REPORT

APOLLO CRYOGENIC SYSTEMS PROGRAMS

MSC/TRW TASK 705-2

NAS 9-8166


DECEMBER, 1970

Prepared for
NATIONAL AERONAUTICS AND SPACE ADMINISTRATION
MANNED SPACECRAFT CENTER
HOUSTON, TEXAS


Prepared by

R. K. M. Seto
C. E. Barton
E. Joseph
P. J. Knowles
J. G. Torian

Approved by:


J. M. Richardson, Head
Engineering Mechanics Section

Approved by:


D. W. Vernon, Manager
Power Systems Department

ABSTRACT

This document is an interim report which describes the progress of MSC/TRW Task 705-2, "Apollo Cryogenic Storage System (CSS) Analysis," Subtask 1, from inception to date. Under this subtask, TRW has developed a simulation program which has the capability of simulating the thermodynamic performance of both the existing Apollo CSS hydrogen and oxygen tanks and the original (Apollo 13 type) CSS oxygen tanks. The operation of the CSS lines and components may also be simulated using a second program. Included in the report are descriptions of the cryogenic storage system and a discussion of the analysis, mathematical formulations and supporting computer subroutines which, when combined, will make up the bulk of the CSS Integrated Systems Program. The Integrated Systems Program development is being accomplished under Subtask 3. Upon completion, the Integrated Systems Program will supercede the programs presented in this report. In their current form, the programs may be used to perform parametric studies of individual tank operation and to perform detailed studies of specific problems related to CSS components and lines.

CONTENTS

	Page
ABSTRACT	i
TABLE OF CONTENTS.	ii
1.0 INTRODUCTION	1
2.0 SYSTEM DESCRIPTION	3
2.1 Cryogenic Storage Tanks	6
2.2 Cryogenic System Components and Lines	9
3.0 ANALYTICAL FORMULATION	14
3.1 Equilibrium Tank Model	14
3.1.1 Tank Model Description	14
3.1.2 Simplified Stratification Analysis	17
3.2 Storage Tank Thermal Model	21
3.2.1 Hydrogen Tank Heat Leak	21
3.2.2 Oxygen Tank Heat Leak	24
3.2.3 Vacuum Annulus Failure	28
3.3 Components and Line Model	34
3.3.1 Model Description	34
3.3.2 Matrix Models	37
3.3.3 Nodal Model	40
3.4 Thermophysical Properties for Oxygen and Hydrogen	52
3.4.1 Oxygen	52
3.4.2 Hydrogen	58
4.0 PROGRAM RESTRICTIONS	60
5.0 RECOMMENDATIONS	62
6.0 REFERENCES	63

CONTENTS (Continued)

	Page
APPENDIX I - NOMENCLATURE	64
APPENDIX II - DERIVATION OF THE RATE OF PRESSURE CHANGE IN THE CSS TANKS	69
APPENDIX III - COMPONENT AND LINE MATRIX MODEL EQUATIONS .	79

TABLES

2.1 CRYOGENIC SYSTEM OPERATIONAL PARAMETERS	7
3.1 COMPARISON OF THE RESULTS OF THE SIMPLIFIED STRATIFICATION ANALYSIS WITH THOSE OF THE BOEING COMPANY	22
3.2 CURVE FIT COEFFICIENTS REPRESENTATIVE OF THE CSS THERMAL ENVIRONMENT	26
3.3 RESIDUAL GAS CONDUCTION CALCULATIONS	30
3.4 CSS TANK HEAT LEAK SUMMARY	31
3.5 OXYGEN SYSTEM CONSTANTS	47
3.6 HYDROGEN SYSTEM CONSTANTS	51
3.7 CONSTANTS FOR STEWART'S EQUATION OF STATE	54
3.8 VARIABLES FOR COMPUTING ISOTHERM DERIVATIVES	55
3.9 VARIABLES FOR COMPUTING ISOCHOR DERIVATIVES	57
3.10 THERMOPHYSICAL PROPERTIES SUBROUTINES	59
A-1 CRYOGENIC TANK PROPERTIES	77
A-2 OXYGEN SYSTEM LUMPED PARAMETER NODAL CONSTANTS	93
A-3 HYDROGEN SYSTEM LUMPED PARAMETER NODAL CONSTANTS	93

ILLUSTRATIONS

2.1 SECTOR IV OF SM MODULE	4
2.2 SECTOR I CSS TANKAGE ARRANGEMENT	5
2.3 CRYOGENIC STORAGE SYSTEM OXYGEN SCHEMATIC	10
2.4 CRYOGENIC STORAGE SYSTEM HYDROGEN SCHEMATIC	11

CONTENTS (Continued)

	Page
3.1 EQTANK PROGRAM GENERAL FLOW DIAGRAM	15
3.2 HYDROGEN TANK HEAT LEAK VAPOR SHIELD FLOW EFFECTS	23
3.3 VARIATION IN HEAT LEAK FOR THE CSS TANKS FOR LOSS OF VACUUM IN THE ANNULUS - AIR LEAKAGE	32
3.4 VARIATION IN HEAT LEAK FOR THE CSS TANKS FOR LOSS OF VACUUM IN THE ANNULUS - HYDROGEN OR OXYGEN LEAKAGE	33
3.5 COMPONENTS AND LINE MODEL FLOW DIAGRAM	38
3.6 EQUIVALENT L/D FOR BEND LOSSES	41
3.7 CHECK VALVE RESISTANCE CHARACTERISTICS	44
3.8 RELIEF VALVE RESISTANCE CHARACTERISTICS	44
3.9 RESTRICTOR PRESSURE DROP	45
3.10 NODAL MODEL NETWORK, H MISSION OXYGEN SYSTEM LINES AND COMPONENTS	46
3.11 NODAL MODEL NETWORK, H MISSION HYDROGEN SYSTEM LINES AND COMPONENTS	50
A-1 LUMPED PARAMETER NETWORK, H MISSION OXYGEN SYSTEM LINES AND COMPONENTS	91
A-2 LUMPED PARAMETER NETWORK, H MISSION HYDROGEN SYSTEM LINES AND COMPONENTS	92

1.0 INTRODUCTION

The objectives of Task 705-2, "Apollo Service Module Integrated Cryogenic Storage System Analysis," are to develop the analytical capability required to:

- a) Develop an integrated mathematical model of the Apollo Cryogenic Storage System (CSS).
- b) Provide support to the redesigned CSS oxygen tank development program.
- c) Predict flight performance of the CSS to verify its adequacy to meet mission requirements.
- d) Carry-out postflight analysis of the CSS to confirm the adequacy of the mathematical model.

To accomplish these objectives, the Task was divided into six subtasks:

Subtask 1 - Basic Cryogenic Tank Program

Subtask 2 - Advanced Cryogenic Tank Performance Program

Subtask 3 - Integrated System Program

Subtask 4 - CSS Oxygen Tank Development Support

Subtask 5 - Preflight Mission Analysis

Subtask 6 - Flight Analysis

This document describes the simulation programs developed under Subtask 1.

In order to predict and study the performance and operation of the Apollo cryogenic storage system, a storage tank model and a lines and components model have been developed. While these models are separate entities at the present time, they will be combined along with other existing programs to comprise the Integrated Systems Program under Subtask 3. Upon completion, the Integrated Systems Program will supercede the programs presented in this report. However, in their current form, the models may be used to perform parametric studies of individual tank operation such as pressure cycle time as a function of tank quantity and flowrates, and detailed studies of

specific problems related to the lines and components such as the thermal response of a quantity of cold gas trapped in a line between a check valve and a shut-off valve, fluid leakage at various places in the lines, etc.

The equilibrium tank model (EQTANK) is capable of simulating the thermodynamic performance of the CSS hydrogen and oxygen tanks. The program accounts for the effects of heat leakage, fan and/or heater operation, duty cycles, and control equipment as well as all significant thermal, elastic, thermoelastic and thermodynamic effects which influence tank performance. A model which correlates the effects of thermal stratification on CSS tank performance is also included. Boundary conditions (input) include the initial state and quantity of the cryogen, flowrate demands of the Environmental Control Subsystem (ECS) and the Electrical Power Subsystem (EPS), component (heater, fan and pressure switch) characteristics, inertial accelerations and spacecraft attitude mode (PTC or inertial hold). The program is designed to simulate a variety of anomalies and failures such as loss of annulus vacuum, fan and/or heater failures, and tank leaks.

The components and lines model (PLMBNG) determines the flow rate apportionment between storage tanks and the thermodynamic state of the constituents at various locations between the source (storage tank) and the points of application (ECS and EPS). Boundary conditions (inputs) include the instantaneous storage tank thermodynamic properties, bay temperatures and EPS and ECS flow requirements. System characteristics are represented by passive distribution system line and component drag characteristics and active component operating characteristics. In addition, provisions are incorporated to simulate a constituent leak at any connection in the system, as well as anomalous operation of all components.

2.0 SYSTEM DESCRIPTION

The Apollo CSS supplies oxygen and hydrogen on a demand basis to the EPS and the ECS. The cryogenic fluids are stored in their supercritical states in tanks located in the Service Module (SM). Each tank is equipped with individual components for filling; venting; quantity, temperature, and pressure measurements; pressure control and relief; and the accompanying displays and controls. For all missions through Apollo 13, the storage system was comprised of two hydrogen tanks and two oxygen tanks. The arrangement of these tanks in Sector IV of the SM is shown in Figure 2.1. For the Apollo 14 Mission the storage system will consist of an additional oxygen tank located in Sector I of the SM making a total of three oxygen tanks and two hydrogen tanks. Subsequent missions will have three hydrogen tanks as well as three oxygen tanks. The additional hydrogen tank will be located in Sector I of the SM. Figure 2.2 presents the tankage arrangement in Sector I.

During nominal operation, the storage system is maintained at a relatively constant pressure with fluid temperature increasing during the mission. Pressure is maintained above the critical pressure in the tanks by the application, either manually or automatically, of electrical heater power. Prior to the Apollo 14 Mission, electrical heat was supplied to the storage tanks in conjunction with destratification fans. However, subsequent to the Apollo 13 oxygen system failure, the system was redesigned to eliminate the fans in the oxygen tanks, although fans are still used in the hydrogen tanks.

The nominal operating pressure of the storage tanks is 245 ± 15 psia and 900 ± 35 psia for the hydrogen and oxygen tanks, respectively.

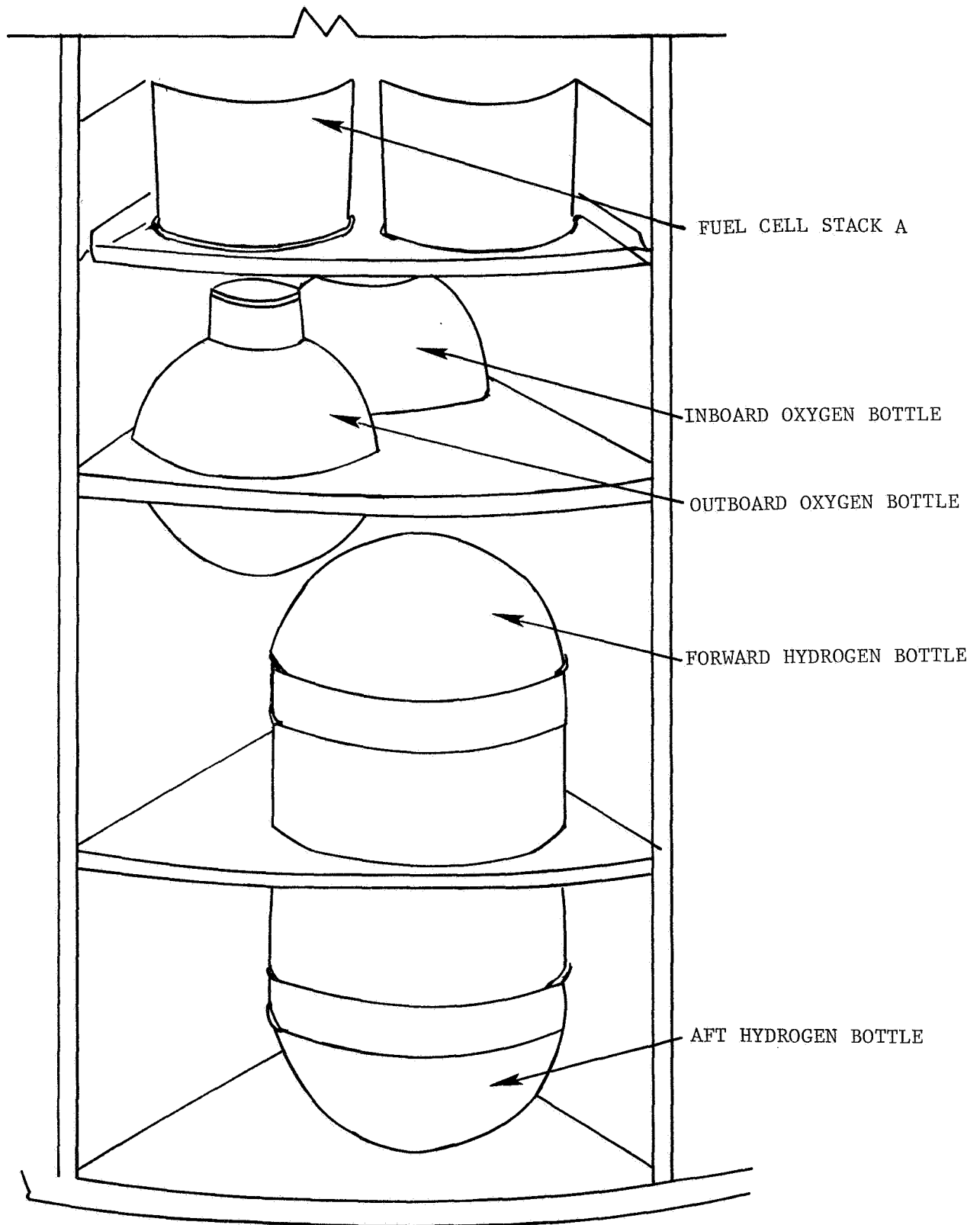


FIGURE 2.1 SECTOR IV OF THE SM MODULE

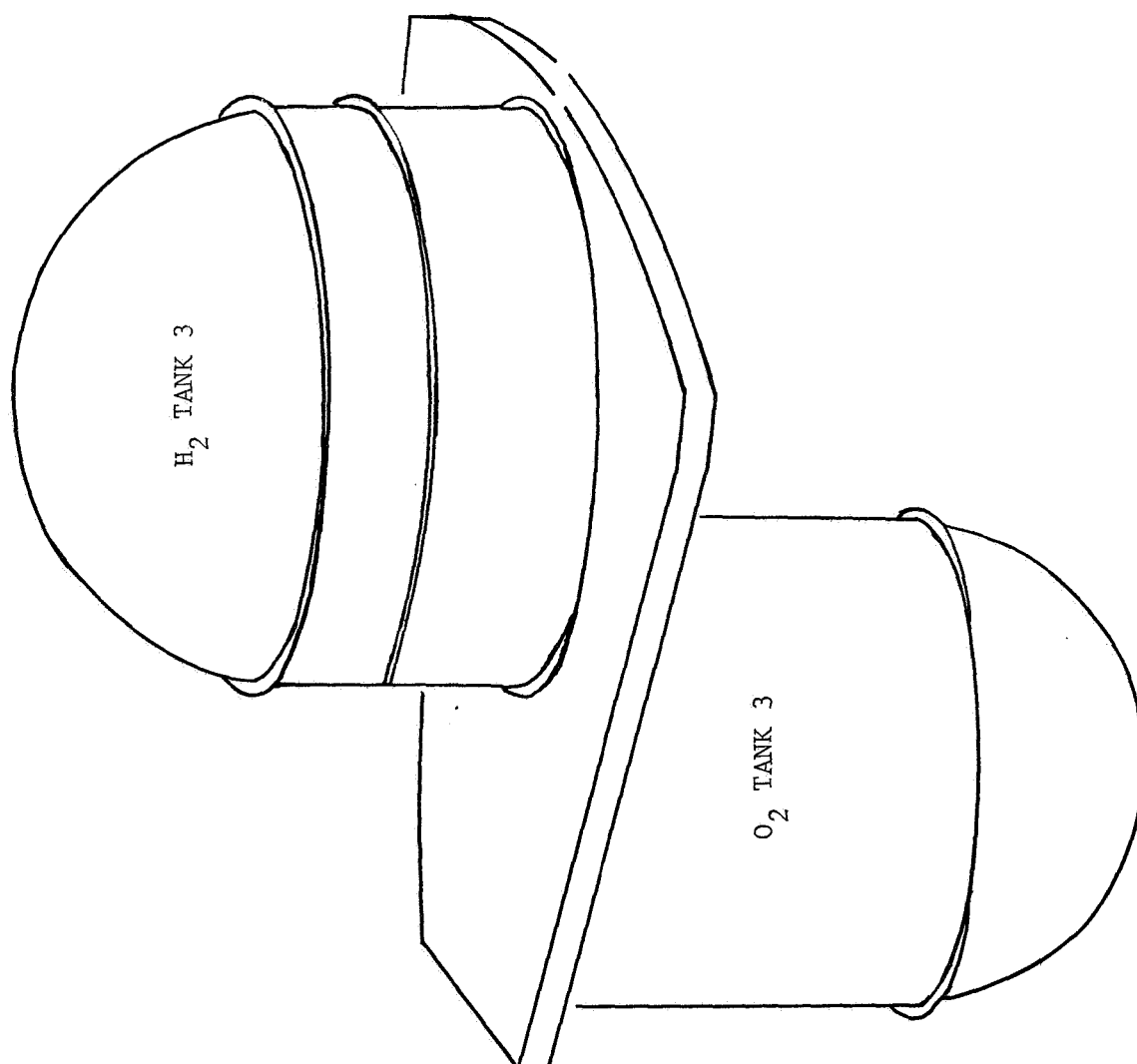


FIGURE 2.2 SECTOR 1 CSS TANKAGE ARRANGEMENT

The fluid flow rate is controlled on a demand basis by the ECS and EPS regardless of the storage systems pressure or operating mode. Under nominal operating conditions there are 29.3 pounds of hydrogen and 330.1 pounds of oxygen loaded into each of the storage tanks. Of these amounts, there are 28.2 pounds of usable hydrogen and 323.5 pounds of usable oxygen. Other pertinent storage system operational parameters are presented in Table 2.1.

2.1 Cryogenic Storage Tanks

A major difference between the oxygen and hydrogen tanks is in the material used in their fabrication. These materials are listed in Table 2.1 and were obtained from Reference 1. In the broad sense, the physical configuration for both tanks is similar in nature and they can be described as a typical unit.

Each tank consists of two concentric spherical shells with thermal insulation in the annular space between the shells. In the oxygen tanks, the insulation supports the pressure vessel. The annulus is also evacuated to improve the thermal barrier qualities. The annulus of each tank is equipped with a vacuum pump to maintain the low pressure required for adequate vacuum insulation, although in flight the oxygen pumps are the only pumps which may be operated. In addition, the pressure vessel supports (hydrogen tank only). fluid lines, and the electrical conduit are located within the evacuated annulus. The exit fluid line is routed through the annulus before exiting from the tank to provide vapor cooling.

Prior to Apollo 13, each tank was equipped with a two element heater and two destratification fans. However, following the Apollo 13 oxygen system failure, the two element heater and destratification fans in the oxygen tanks were removed and replaced with a three element heater. In addition, the heater

TABLE 2.1

CRYOGENIC SYSTEM OPERATIONAL PARAMETERS

	<u>Hydrogen</u>	<u>Oxygen</u>
TANK MATERIAL	5 Al-2.5 Sn ELI t1	Inconel 718
TANK WEIGHT (PER TANK)		
Empty (Approx)	80.00 lb.	90.82 lb.
Usable Fluid	28.15 lb.	323.45 lb.
Stored Fluid (100% indication)	29.31 lb.	330.1 lb.
Residual	4%	2%
Maximum Fill Quantity	30.03 lb.	337.9 lb.
TANK VOLUME (PER TANK)	6.80 ft ³	4.75 ft ³
TANK FLOW RATE (PER TANK)		
Max. for 10 Minutes	1.02 lbs/hr	4.03 lbs/hr
Max. for 1/2 hour	-----	10.40 lbs/hr
Relief Valve Max Flow	6 lbs/hr @ 130°F	26 lbs/hr @ 130°F
TANK PRESSURIZATION		
Heaters elements per tank	2	3
Flight Resistance	78.4 ohms per element	18.45 ohms per element
Nominal Voltage	28 V DC	28 V DC
Power	10 watts per element*	42.5 watts per element*
Total Heater Heat Input Per tank	68.2 BTU/Hr	434.8 BTU/Hr
Ground Resistance	78.4 ohms per element	18.45 ohms per element
Voltage	28 V DC	28 V DC
Power	10 watts per element*	42.5 watts per element*
Total Heater Heat Input Per Tank	68.2 BTU/Hr	434.8 BTU/Hr
* Conversion Factor: 1 watt = 3.41 BTU/Hr		

TABLE 2.1 (Continued)

	<u>Hydrogen</u>	<u>Oxygen</u>
Pressure Switch		
Open Pressure Max.	260 psia	935 psia
Close Pressure Min.	225 psia	865 psia
Deadband Min.	10 psia	30 psia
Destratification Motors (2 Motors Per Tank)		
Voltage	115/200 V	None
	400 cps	None
Power - Average	3.5 watts per motor*	None
Total Average Motor Heat Input Per Tank	23.8 BTU/Hr	None
SYSTEM PRESSURES		
Normal Operating	245 ±15 psia	900 ±35 psia
Spec Min. Dead Band of Pressure Switches	10 psi	30 psi
Relief Valve Note:	Relief Valves are referenced to environmental pressure, therefore pressure at sea level (psig) will be the same value in vacuum (psia)	
Crack Min.	273 psig	938 psig
Full Flow Max.	285 psig	1010 psig
Reseat Min.	268 psig	865 psig
Outer Tank Shell Burst Disc		
Nominal Burst Pressure	90 ⁺¹⁰ / ₋₂₀ psid	75 ±7.5 psid
SYSTEM TEMPERATURES		
Stored Fluid	-425 to 80°F	-300 to 80°F
*Conversion Factor: 1 watt = 3.41 BTU/Hr		

thermostat for protection against high heater temperatures has been removed and replaced with a temperature sensor. The new sensor is located on the heater tube. Another temperature sensor is located above the capacitance probe and measures the bulk fluid temperature. Electrical lines leading into the redesigned oxygen tank have also been sheathed to reduce the fire hazard.

2.2 Cryogenic System Components and Lines

Figures 2.3 and 2.4 are schematics of the component and line configurations for the Apollo 14 oxygen and hydrogen systems, respectively, showing the relative locations of the components which make up the system. In general, the system is composed of lines, valve modules, flow filters and flow restrictors. For missions prior to Apollo 14, the system valve modules for both the hydrogen and oxygen systems each contained two relief valves, two pressure transducers, two pressure switches and one check valve. For Apollo 14, a half valve module was added for oxygen tank 3 and contains one relief valve, one pressure switch, and a check valve. A solenoid operated shutoff valve was also added between oxygen tanks 2 and 3.

The relief valves in these modules are a gradual opening differential pressure poppet type which assure the lowest possible leakage and have virtually zero delta pressure between crack and full flow. These valves are designed to be unaffected by back pressure in the downstream plumbing and are temperature compensated over the full range of fluid temperatures which may occur.

The pressure transducers are absolute pressure devices which utilize bonded strain gauges to produce millivolt signals to the signal conditioner. The signal conditioner is integral to the transducer with a 0 to 5 VDC output linearly proportioned to tank pressure. The transducers can operate at

Figure 2.3 Cryogenic Storage System Oxygen Schematic

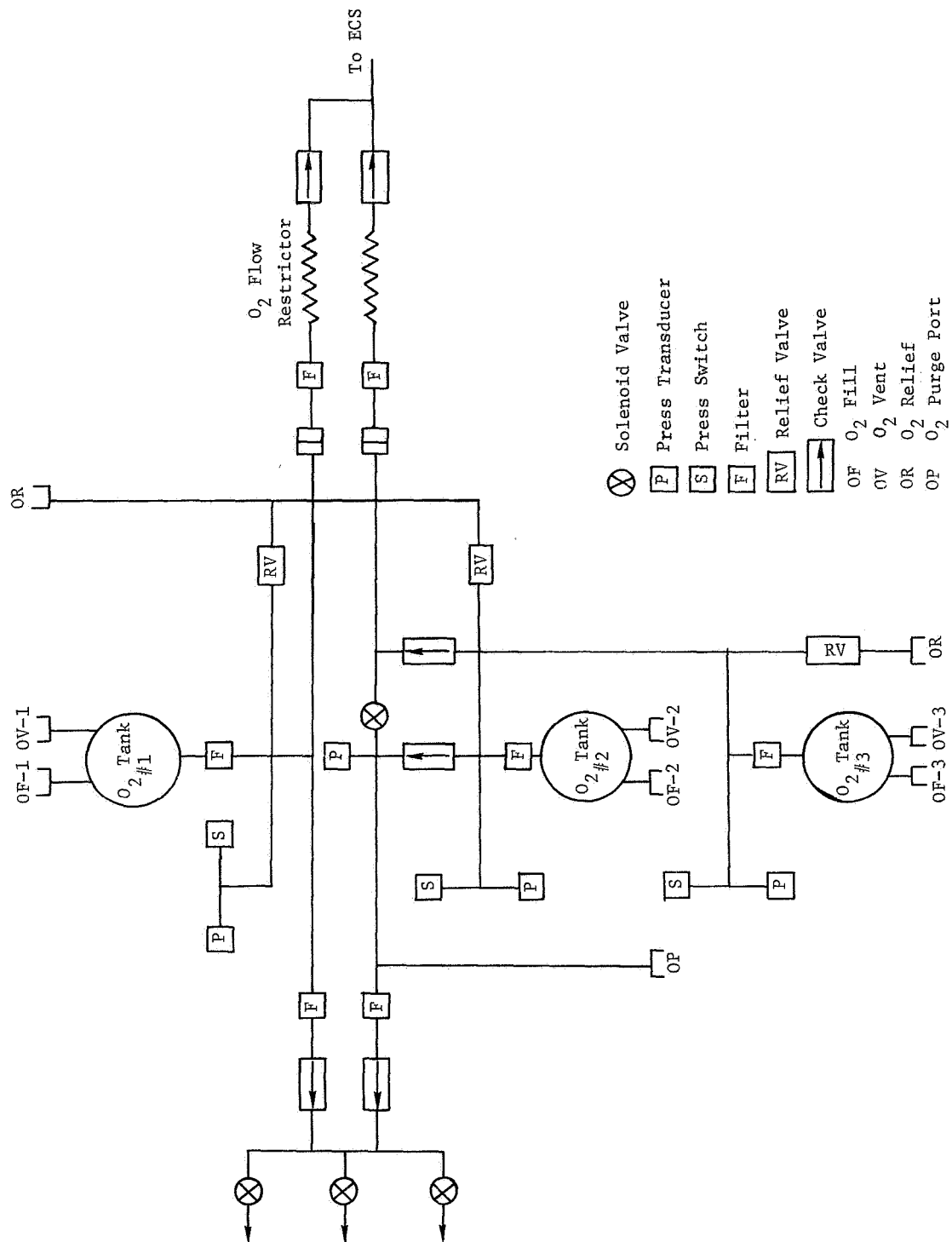
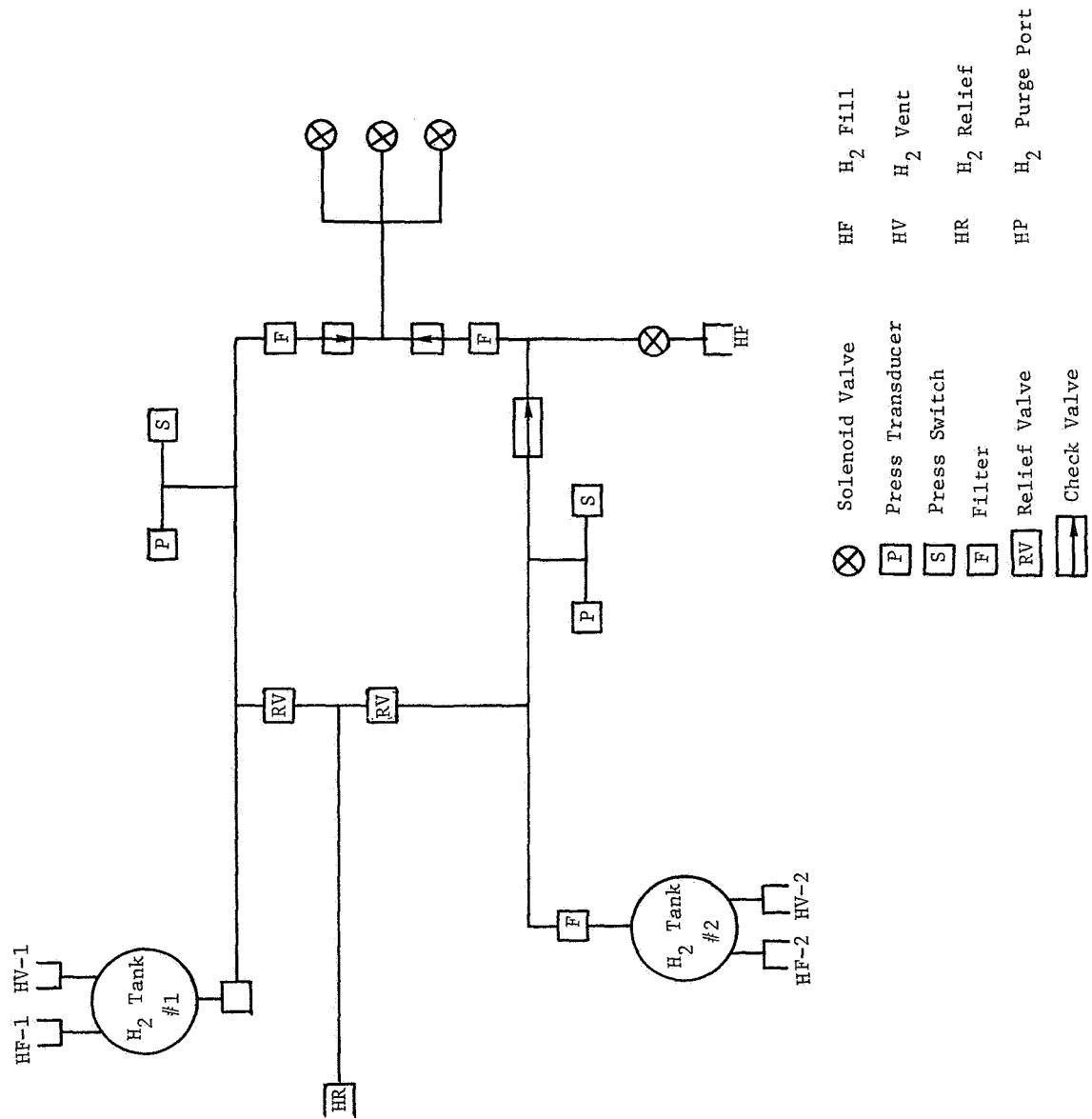


Figure 2.4 Cryogenic Storage System Hydrogen Schematic



environmental temperatures as low as -80°F and are capable of supplying a continuous readout of pressure over the specified range with a maximum error of $\pm 2\text{-}1/2$ percent of full scale.

The pressure switches are single-throw, single pole absolute pressure devices which may be used to control the motor switches which activate the destratification motors and/or tank heaters. These switches have been used successfully in an environment of -400°F .

The check valve is a spring loaded poppet type and is designed to open at a differential pressure of approximately 1 psi. The valve seat has a large area to prevent chattering during flow in the normal direction and to help obtain a positive seal if pressurized in the reverse direction.

The fuel cell valve module for the hydrogen system consists of two check valves and three solenoid operated valves in one valve body. The check valves are a dual seat type which allow the main passage to be full open and the auxiliary passage barely cracked at low flows. At high flows, both the main and auxiliary passages are completely open. The solenoid valves are poppet latch type and are actuated by a magnetic armature suspended on a Bellville spring. Opening and closing coils on both sides of the armature actuate the valve. The valves open against pressure and pressure helps to seal the valve against leakage when closed to flow in the normal flow direction.

For the oxygen system, the fuel cell valve module contains check valves similar to those in the hydrogen fuel cell valve module. However, subsequent to Apollo 13, the solenoid valves have been taken out of the module and mounted externally and upstream of the flow transducers to the fuel cells.

The oxygen and hydrogen inline filters consist of several chemically etched discs stacked in a cartridge. They are rated at 5 microns nominally and 12 microns absolute with a capacity to contain .25 grams contaminant.

Several components have been added to the CSS for missions subsequent to the Apollo 14 ("J" type missions). A half valve module containing a relief valve, a pressure switch, and a check valve has been added for the third hydrogen tank. There are three oxygen restrictors in the ECS for J type missions versus two for other Apollo missions. The third restrictor line is a branch of the oxygen tank 2 ECS supply line and reconnects downstream of the junction of the other two restrictor lines. This restrictor line includes a filter and check valve.

3.0 ANALYTICAL FORMULATION

The following sections discuss the analytical formulations of the two programs which model the tanks and the components and lines as well as two supporting subroutines. Section 3.1 describes the equilibrium tank program. In order to compute the heat leak to the tanks, it was necessary to develop a storage tank thermal model which is described in Section 3.2. The components and lines model is discussed in Section 3.3. Finally, a subroutine was developed to provide the other models with oxygen and hydrogen thermophysical properties as required. This model is described in Section 3.4.

3.1 Equilibrium Tank Model

The Equilibrium Tank Model (EQTANK) computer program was developed to simulate the thermodynamic performance of the Apollo CSS hydrogen and oxygen tanks. Any combination of up to three hydrogen and three oxygen tanks may be simulated. Both the Apollo 13 type oxygen tank as well as the redesigned tank are modeled.

3.1.1 Tank Model Description

The EQTANK program simultaneously updates the thermodynamic state in each storage tank of the CSS based on control equipment operation, flowrates, tank characteristics, heat leaks, and trajectory data. It is assumed that thermodynamic equilibrium exists in the tanks at all times. Figure 3.1 presents an overall flow diagram of the model.

The basic equation for the model determines the rate of change of pressure with respect to time and is given by:

$$\frac{dP}{dt} = \frac{\frac{\theta \phi}{V} \dot{m} \left[1 - \frac{3\alpha_{\rho_o} \frac{\partial T}{\partial P}}{V(1+3\alpha_{\rho_o} \frac{\partial T}{\partial P})} \right] + \frac{\phi}{V} q}{\frac{\theta \phi \rho_o}{1+3\alpha_{\rho_o} \frac{\partial T}{\partial \rho_o}} \left[\frac{V_2}{VNP} + \frac{3r}{2\beta Y} (1-u) + 3\alpha \frac{\partial T}{\partial P} \right]} \quad (1)$$

The flowchart is divided into two main sections by a dashed line:

- THIS PROGRAM SEGMENT COMPUTES TIME INCREMENT** (Left side):
 - Starts with **Data** pointing to **T(I,J)**.
 - T(I,J)** points to a box containing **IHTRD** and **IFAND**.
 - This box points to **HTON(I,J)** and **CYTIM(I,J)**.
 - This points to **IFAN(I,J)** and **IHIRC(I,J)**.
 - This points to **Q(I,J)**.
 - Q(I,J)** points to **QLEAK(I,J)** and **TEXIT(J)**.
 - QLEAK(I,J)** and **TEXIT(J)** point to **PPPR**, **PPPT**, **PHID**, and **THETAD**.
 - PPPR**, **PPPT**, **PHID**, and **THETAD** point to **P(TPP(I,J))**.
 - P(TPP(I,J))** points to **PTPRO**.
 - PTPRO** points to **DPDT(I,J)** and **DPDTE**.
 - DPDT(I,J)** and **DPDTE** point to **DTG(I,J)**.
 - DTG(I,J)** points to **PNEXT**.
 - PNEXT** points to **TLIMIT(I,J)**.
 - TLIMIT(I,J)** points to **TGALC**.
 - TGALC** points to **ISHD**.
 - ISHD** points to **ISFD**.
 - ISFD** points to **PBAR**.
 - PBAR** points to **RHOBAR**.
 - RHOBAR** points to **TBAR**.
 - TBAR** points to **PPPR**, **PPPT**, **PHI(I,J)**, and **THETA(I,J)**.
 - PPPR**, **PPPT**, **PHI(I,J)**, and **THETA(I,J)** point to **P(TPP(I,J))**.
 - P(TPP(I,J))** points to **PTPRO**.
 - PTPRO** points to **DPDT(I,J)**.
 - DPDT(I,J)** points to **P(I,J)**.
 - P(I,J)** points to **G**.
 - G** points to **ACCELN(I,J)**.
 - ACCELN(I,J)** points to **PCT**.
 - PCT** points to **DPCDT**.
 - DPCDT** points to **PC(I,J)**.
 - PC(I,J)** points to **IPS(I,J)**.
 - IPS(I,J)** points to **WT(I,J)**.
 - WT(I,J)** points to **RHO(I,J)**.
 - RHO(I,J)** points to **FTANK(I)**.
 - FTANK(I)** points to **OUTPUT**.
 - OUTPUT** points to **TIME CHECK**.
- THIS PROGRAM SEGMENT UPDATES STATES OF ALL TANKS** (Right side):
 - Starts with **TLIMIT(I,J)** pointing to **ISFD**.
 - ISFD** points to **ISHD**.
 - ISHD** points to **ISFD**.
 - ISFD** points to **PBAR**.
 - PBAR** points to **RHOBAR**.
 - RHOBAR** points to **TBAR**.
 - TBAR** points to **PPPR**, **PPPT**, **PHI(I,J)**, and **THETA(I,J)**.
 - PPPR**, **PPPT**, **PHI(I,J)**, and **THETA(I,J)** point to **P(TPP(I,J))**.
 - P(TPP(I,J))** points to **PTPRO**.
 - PTPRO** points to **DPDT(I,J)**.
 - DPDT(I,J)** points to **P(I,J)**.
 - P(I,J)** points to **G**.
 - G** points to **ACCELN(I,J)**.
 - ACCELN(I,J)** points to **PCT**.
 - PCT** points to **DPCDT**.
 - DPCDT** points to **PC(I,J)**.
 - PC(I,J)** points to **IPS(I,J)**.
 - IPS(I,J)** points to **WT(I,J)**.
 - WT(I,J)** points to **RHO(I,J)**.
 - RHO(I,J)** points to **FTANK(I)**.
 - FTANK(I)** points to **OUTPUT**.
 - OUTPUT** points to **TIME CHECK**.

EQ TANK PROGRAM

The nomenclature used is defined in Appendix I.

Equation (1) is derived in Appendix II and accounts for variations in tank volume due to fluid pressure and temperature excursions. The expression further accounts for the effect on the rate of change of pressure due to the attached fill and vent lines which act as small gas reservoirs. All terms in the relation for pressure rise or decay rate may be determined from the CSS system and fluid thermodynamic properties. The variables r , V , β , Y , v , V_2 and α are obtained from tank material and geometric characteristics. The thermodynamic variables θ , ϕ , ρ_0 , $\frac{\partial T}{\partial P}$, P , and $\frac{\partial T}{\partial P}$ are obtained from the Thermophysical Properties Subroutine discussed in Section 3.4. The total heat input rate, q , is the sum of the heat leak calculated by the Storage Tank Thermal Model Subroutine (Section 3.2) and the heat input resulting from the operation of tank heaters and/or fan motors. The mass flowrate, \dot{m} , is an input variable to the EQTANK Program. The gas compression process in the tank fill and vent lines is assumed to be isothermal, so the polytropic exponent, N , is currently assumed to be 1.0 for both oxygen and hydrogen.

The program may be divided into two sections. The first section determines the maximum time increment over which all tanks may be simulated. The second section uses this time increment to update the state of the fluid in each tank corresponding with the conditions which prevail at the end of the time increment.

The time increment depends on the rate of change of pressure and the operation of the pressure switches in each tank. Equation (1) is used to determine when a tank pressure will reach a specified excursion (currently 15 psi) from its initial state or when a pressure control limit will be reached for the tank. The shorter of these two time increments is defined as the maximum dynamic simulation time increment for the tank. Dynamic simulation time

increments for all tanks are compared and the smallest one is chosen as the total tank system dynamic simulation time increment. This time increment is then compared with a user specified increment and the lesser is selected as the time increment for use in updating the state of all cryogenic tanks.

Upon the determination of the time increment, the thermodynamic state of the fluid in each tank is updated. The average pressure for the time interval is determined from the initial tank pressure, the initial pressure rise (or decay) rate, and the length of the time interval. The average density for the time interval is determined from the tank volume, the initial weight of cryogen in the tank, and the flowrate. Using these averaged thermodynamic properties, the average pressure change rate is determined using Equation (1) for each tank. The average pressure change rate and flowrate are then used to update the pressure and density at the end of the time interval. Finally fluid temperature is obtained using the Thermophysical Properties Subroutine.

In addition to updating the state of each of the cryogenic tanks, the second portion of the EQTANK program performs three other operations. The tank pressure at the end of the time interval is compared with the limit pressures for the tank pressure switch, and the pressure switch state changed if necessary. The collapse pressure potential (Section 3.1.2) for each oxygen tank is estimated from knowledge of time interval length, tank state, acceleration level, and tank flow rate. The last mathematical operation in the EQTANK program is to determine the additional flowrates required by the fuel cells to provide power for all electrical equipment operating in the tanks at the end of the time interval.

3.1.2 Simplified Stratification Analysis

As a result of the CSS failure during Apollo 13, considerable effort has been devoted to the analysis of single phase cryogenic storage under

low accelerations. The purpose of the analysis was to evaluate the potential pressure collapse that could occur in the tank due to thermal stratification of the fluid. A large pressure collapse could undesirably change the single phase fluid to a two phase fluid. During the Apollo 7 Mission, flight tests were performed which demonstrated that pressure collapse was not significant in the hydrogen tanks. Therefore, the potential collapse pressure (difference between the instantaneous pressure value and the value that would result from sudden complete mixing of the fluid) was assumed to be negligible for hydrogen and the analytical investigations have been limited to the oxygen tanks.

Localized heat addition from heaters placed in the oxygen storage vessels to assist the fluid expulsion process results in local hot gas pockets which cause density gradients to form in the fluid. Since the vessel pressure is determined by the warmer fluid, mixing of the fluid can result in a pressure collapse. The stratification process which leads to potential collapse pressures is a result of poor conductive heat transfer properties of oxygen coupled with limited mechanical and convective mixing due to low acceleration.

Mathematical models of the thermodynamic processes which take place in the oxygen storage vessels must be very detailed and, as a result, require a large amount of computer time in order to simulate the fluid stratification process and determine the potential pressure collapse. For this reason, a simplified oxygen fluid stratification analysis model was constructed, based on detailed simulations performed by C. K. Forester of the Boeing Company, Seattle, Washington (Reference 2). This simplified model requires only a fraction of the computer time needed for the detailed model and generally provides accuracies on the order of 10% as compared to the results of the detailed model. Thus, it was practical to incorporate the simplified model into the EQTANK program. The EQTANK program uses a correlation model to estimate the magnitude and effects of rapid destratification. The exact form of the oxygen potential pressure collapse model resulted from an analysis of the numerical studies obtained from Boeing.

Logically, the collapse pressure potential for any Apollo CSS tank should be dependent on the local acceleration, fluid flow rate and the fluid quantity histories of the tank. The dependence on histories rather than instantaneous values suggests that an integral approach is appropriate. This is reinforced by the fact that the operation of a CSS tank depends upon the path or history of the thermodynamic process. The problem of finding potential collapse pressure, then, is to determine and integrate the time derivative of the potential collapse pressure.

The effects of acceleration level on potential collapse pressure can be practically detected only between the levels of 10^{-7} and 10^{-3} g. An acceleration level of 10^{-3} g will rapidly destratify a normally functioning Apollo CSS tank, while actual accelerations of less than 10^{-7} g are difficult to obtain in manned spacecraft due to astronaut motion and equipment operation. The variation of potential collapse pressure growth rate over the acceleration range of interest changes by a factor of approximately ten. The effects of small acceleration changes on the potential collapse pressure growth rate are more pronounced at lower accelerations. Both of the previous observations suggest that a logarithmic variation of potential collapse pressure growth rate with acceleration is appropriate for a correlation model. The final dependence of potential collapse pressure on acceleration was found to vary as the square of the logarithm between accelerations of 10^{-7} g and 10^{-3} g with a value of one at less than 10^{-7} g and a value of zero at accelerations greater than 10^{-3} g.

The effect of fluid flow rate on stratification in single phase cryogenic tanks is to increase the magnitude of the potential collapse pressure. The potential collapse pressure increases more rapidly at high flow rates than at low flow rates because the heat input to the fluid does not have time to diffuse by conduction throughout the tank. This leads to increased density

and temperature variations within the tank. These variations in the fluid properties bring about an increase in the potential collapse pressure. A linear dependence on flow rate was incorporated into the EQTANK correlation model for potential collapse pressure.

The effect of the quantity of oxygen in a tank on the buildup of potential collapse pressure within the tank may be understood by considering two heat transfer effects in high density single phase oxygen. First, because of the proximity of the oxygen to the two-phase boundary, conductive heat transfer is low in high density oxygen at the operational pressures in the oxygen tanks. Second, and perhaps more important, the thermal diffusivity or effective heat propagation rate in fluids is inversely proportional to the density of the fluid. Thus, thermal energy input to high density fluids tends to remain where it was introduced rather than diffusing throughout the entire fluid mass. A linear dependency of potential collapse pressure rate of fluid density or tank quantity is used in the program. The relation is displaced from the origin such that no potential collapse pressure buildup can occur at tank quantities less than 37.5 percent, since below that quantity, effects of stratification are negligible. A linear collapse pressure dependency on tank quantity was selected to give a collapse pressure buildup rate consistent with results of the Boeing study.

It was determined that a separable form of the collapse pressure rise rate correlation equation could be used to describe the simultaneous dependence of the potential pressure collapse on acceleration, flowrate, and tank quantity. A step function H is incorporated into the acceleration and quantity dependences to affect a good agreement of the correlation model over the acceleration region of interest. The final expression for the time derivative of potential collapse pressure used in the EQTANK program is:

$$\frac{dP_c}{dt} = \left\{ H(10^{-7} - g_c) + [H(g_c \cdot 10^{-7}) - H(g_c \cdot .001)] \frac{\ln_{10}^2 \left(\frac{.001}{g_c} \right)}{16} \right\} \\ \left\{ \dot{m}[H(\% - 37.5)] \cdot .1792(\% - 37.5) \right\}$$

A comparison of the results of the correlation model and those obtained numerically by Boeing is presented in Table 3.1.

3.2 Storage Tank Thermal Model

The CSS consists of dewar vessels for the storage of both oxygen and hydrogen. Insulation for these vessels is provided by a vacuum jacket which consists of a space filled with insulating material coupled with a vapor cooled shroud (VCS). The heat leak into the storage vessels under nominal operating conditions is primarily a function of the flowrate through the VCS and the temperature in the bay. The bay temperature depends to a large extent upon whether the vehicle is in an inertial hold mode or a passive thermal control mode. The effect of vacuum loss in the jacket is to increase the heat leak into the storage vessel.

The vehicle thermal model was developed as a subroutine for inclusion in the EQTANK model and is essentially made up of three parts. These include separate heat leak calculations for the oxygen and hydrogen tanks and a part for computing the heat leak under various loss of vacuum conditions.

3.2.1 Hydrogen Tank Heat Leak

The heat leak to the hydrogen tank under nominal operating conditions is computed in the thermal model using data taken from the Apollo Flight Support Handbook (Reference 1). This data, presented in Figure 3.2, is a correlation of estimated heat flux as a function of the fluid expulsion rate and the quantity of fluid remaining in the tank. The origin of this data, however, is not known and the effect of temperature in the bay on the heat flux has not been included. Since the outer wall temperature is not taken into account, the mission mode cannot be considered in the calculation

TABLE 3.1

COMPARISON OF THE RESULTS OF THE SIMPLIFIED STRATIFICATION ANALYSIS
WITH THOSE OF THE BOEING CO.

GROWTH RATE OF POTENTIAL COLLAPSE PRESSURE				
Acceleration	Mass Flow Rate (lbm/hr)	Tank Quantity (%)	Simplified Correlation Results (psia/hr)	Boeing's Numerical Results (psia/hr)
2.6	1.23	52.	1.33	1.43
0.5	.92	75.	4.21	3.86
2.6	.85	12.	0.	0.
0.1	1.45	96.	15.20	20.29
0.1	.87	95.	9.	7.
0.5	.94	75.	4.30	4.25
0.5	4.50	97.	32.70	32.
0.5	4.50	75.	20.60	9.25
0.5	4.50	52.	8.	8.5
0.5	4.50	38.	.27	1.0
0.5	4.50	23.	0.	0.

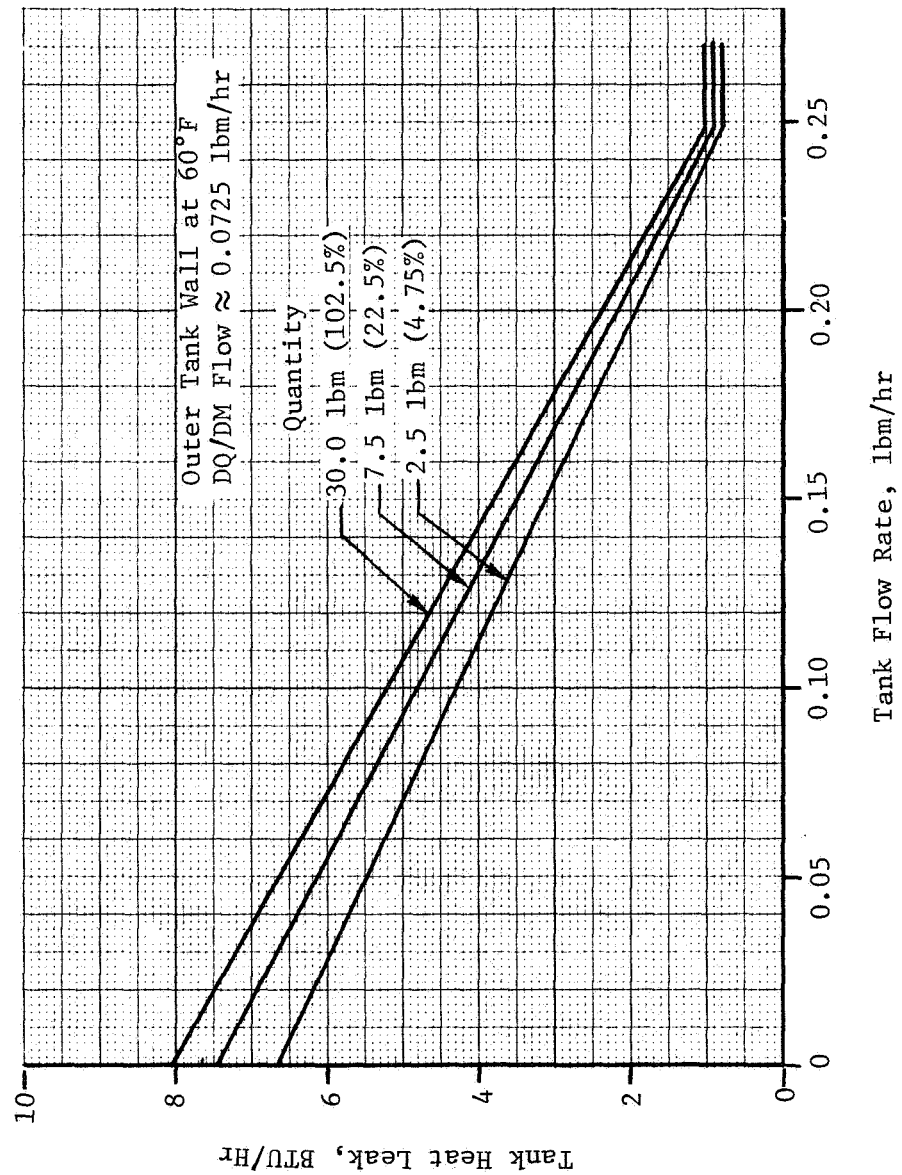


Figure 3.2 Hydrogen Tank Heat Leak Vapor Cooled Shield Flow Effects

of the hydrogen tank heat leak. In addition, the discontinuity occurring in the curves at a flow rate of 0.25 lbm/hr does not appear reasonable. Although the correlations presented in Figure 3.2 do not appear to adequately define the heat leak into the hydrogen tanks, it is the only data currently available. However, if additional data becomes available, the hydrogen tank heat leak correlations used in this portion of the program may be updated easily.

3.2.2 Oxygen Tank Heat Leak

The heat leak into the oxygen tanks during nominal operating conditions is computed in the thermal model using empirical data correlations developed by the Beech Aircraft Company (Reference 3). These correlations relate the heat transfer into the oxygen tank with the temperature of the oxygen in storage, the oxygen expulsion rate and the tank outer wall temperature. These correlations are given by the following equations:

$$QR = AL1 (TOS^{2.5} - TVCS^{2.5}) - \dot{m} (HVCS - HPV) \quad (2)$$

$$QR = AL2 (TVCS^{2.5} - TPV^{2.5}) \quad (3)$$

$$q = AL3 (TOS - TPV) + .9QR \quad (4)$$

The value of the constants which apply to Equations (2), (3), and (4) are as follows:

$$\text{Redesigned Tank: } AL1 = 1.2114 \times 10^{-5} \text{ BTU/HR}^{\circ R^{2.5}}$$

$$AL2 = .95779 \times 10^{-5} \text{ BTU/HR}^{\circ R^{2.5}}$$

$$AL3 = .037753 \text{ BTU/HR}^{\circ R}$$

The amount and temperature of the oxygen in storage is computed in another portion of the EQTANK program and used as input for the thermal subroutine.

The outer wall tank temperature is computed within the thermal subroutine through a series of data curve fit correlations. The data for these

correlations was derived from the Thermal Mathematical Model (TMM) of the Apollo Service Module developed by TRW under MSC/TRW Task ASPO-62C. This program is composed of over 800 lumped parameters that constitute a thermal network specifically formatted for solution with the SINDA Multi-Option computer program. This program uses as input the results of the Apollo Spacecraft External Radiation Heating Program, which computes the solar absorption, the solar albedo and planetary radiation absorbed by the Service Module (SM) for orbital and translunar flight, to compute the heat conductance through the SM structure. The SM program obtains its boundary conditions for a specific mission from trajectory and attitude tapes. The TMM program takes into account mass changes to the SM (such as SPS and RCS propellant usages) and internal heat loads (such as ECS and EPS). The program presently determines the temperature of each oxygen and hydrogen tank surface assuming a uniform internal tank temperature, which increases with mission time.

For use in the thermal subroutine, the temperature computed for the surface of the oxygen tanks by the TMM has been averaged for each tank and curve fit as a function of time. The form of the resulting curve fit equations is::

$$T = a_0 + a_1x + a_2x^2 + a_3x^3$$

where x is the time argument.

These curve fit equations have been implemented into the thermal subroutine, thus, enabling the tank outer wall temperature to be estimated, taking into account the mission mode (inertial hold or passive thermal control) in addition to the sun look angle. The coefficients for the polynomial curve fit equations are shown in Table 3.2 together with the inherent standard deviation introduced with their use. The first six curves presented in this table are used in the thermal subroutine. Temperatures for the remaining nodes in Table 3.2 will

TABLE 3.2

CURVE FIT COEFFICIENTS REPRESENTATIVE
OF THE CSS THERMAL ENVIRONMENT

Mission Mode	Node	Curve	a_0 (°F)	a_1 (°F/Hr)	a_2 (°F/Hr ²)	a_3 (°F/Hr ³)	Standard Deviation (°F)	Time Argument	
								t+3 (Hrs)	$\frac{t+3}{t+3-1}$ (Hrs)
PTC	Tanks 1&2	1	46.152	35.715	105.97	-38.106	0.992		X
PTC	Tank 3	2	25.164	73.761	202.92	-112.08	1.082		X
Hot Soak	Tanks 1&3	3	60.0	4.44	0	0	-	X	
Hot Soak	Tank 2	4	58.523	31.715	2.57	.1277	2.750	X	
Cold Soak	Tanks 1&3	5	-15.824	368.40	485.5	232.26	1.428		X
Cold Soak	Tank 2	6	-61.812	549.39	650.84	283.34	3.520		X
PTC	150	7	51.8	286.2	-1562.	2557.	1.03		X
	153	8	83.5	-30.0	-555.9	1583.	.4		X
	151	9	52.0	-113.3	608.9	-744.5	.8		X
	154	10	54.2	-80.9	1302.	-3326.	1.0		X
	156	11	46.6	14.1	241.5	-583.8	0.4		X
	157	12	99.8	129.5	-1925.	3671.	0.7		X
	152	13	117.6	120.5	-2103.	3961.	0.6		X
	158	14	88.1	24.1	-1110.	2633.	0.5		X
	159	15	69.0	65.1	-591.9	1212.	0.2		X
PTC	155	16	46.0	49.0	-45.8	51.6	0.3		X
Hot Soak	150	17	31.87	513.11	-2421.	3633.	.975		X
	153	18	109.77	-12.09	-1101.	2344.	.386		X
	151	19	115.34	-156.	262.	-1056.	.41		X
	154	20	123.	-335.	2378.	-6127.	1.129		X
	156	21	104.2	-58.04	-460.	597.	.3		X
	157	22	130.1	76.16	-1973.	3463.	.6		X
Hot Soak	152	23	137.2	229.7	-3298.	6029.	.7		X

$$T = a_0 + a_1X + a_2X^2 + a_3X^3 \quad \text{where } X = \text{time argument}$$

MODE	NODE	CURVE	a_0 (°F)	a_1 (°F/Hr)	a_2 (°F/Hr ²)	a_3 (°F/Hr ³)	Standard Deviation (°F)	Time Argument	
								t+3 (Hrs)	$\frac{1}{t+3-1}$ (Hrs)
Hot Soak	158	24	108.6	91.3	-1988.	4104.	.36		X
	159	25	54.2	-2.1	313.8	-502.	.34		X
	155	26	114.2	-125.8	185.9	-931.	.52		X
Cold Soak	150	27	42.75	334.	-1640.	2600.	1.0		X
	153	28	55.2	-75.7	347.3	67.2	.85		X
	151	29	16.4	-45.1	950.6	-4120.	.85		X
	154	30	-5.35	315.	240.	-2098.	.966		X
	156	31	-4.96	275.	44.4	-961.	.5		X
	157	32	83.5	166.2	-1736.	3203.	.5		X
	152	33	97.5	187.0	-1946.	3427.	.6		X
	158	34	60.7	25.5	-409.	1264.	.45		X
	159	35	144.4	-324.	-416.	2155.	.3		X
Cold Soak	155	36	-7.3	326.1	-362	-70.7	.5		X
	150	37	-35806.	1143.	-12.1	.04	5.4	X	
	153	38	13096.	-420.	4.5	-.016	1.06	X	
	151	39	45.	0	0	0	-	X	
	154	40	80.	0	0	0	-	X	
	156	41	16000.	-520.	5.65	-.02	2.2	X	
	157	42	80.	0	0	0	-	X	
	152	43	-29911.	943.9	-9.90	.035	.48	X	
	158	44	70.	0	0	0	-	X	
Lunar Orbit	159	45	-12853	440.5	-4.97	.018	1.2	X	
	155	46	19283	-627.5	6.8	-.025	2.6	X	

TABLE 3.2 (Cont'd)

be used in lines and components model when the Integrated Systems Program is completed.

The first step in the oxygen tank thermal subroutine is to determine if the tank vacuum jacket is nominal or has failed. If the vacuum jacket has failed, the heat leak is computed using methods discussed in Section 3.2.3. If the tank is in nominal operating condition, the mission mode is checked and the tank outer wall temperature is determined using the correlated results from the TMM program. A Newton-Raphson iteration technique is used to adjust the time argument of each curve to determine the outer wall temperature. These temperatures are then adjusted to account for the sun look angle. The temperature of the fluid in the VCS is then computed from the temperature of the fluid in storage and the outer wall temperature, using an iteration scheme. Once the temperature of the VCS fluid has been determined, the heat flux is computed using Equations (2), (3), and (4).

3.2.3 Vacuum Annulus Failure

The nominal pressure in the tank annulus under the design vacuum condition is approximately 10^{-7} torr (mm Hg). Depending upon the type of failure, the annulus pressure in the failed condition will be somewhere between the nominal pressure and the annulus burst disc pressure. Burst disc pressures for the oxygen and hydrogen tanks are approximately 75 and 80 psia, respectively. Within these pressure bounds, gas in the annulus may exist in either rarefied or continuum regimes. Although criteria for determining the gas regime is not exact, it is based primarily on the ratio of the molecular mean free path to the amount of space available for molecular motion. This ratio is defined as the Knudsen number (K_n). For values of $K_n < 0.01$ the gas is normally treated as continuum flow, while for values of $K_n > 1.0$ the gas is assumed to be in the rarefied regime. For the CSS tanks, an annulus pressure on the order of 10^{-3} psia represents the transition between the two regimes.

The type of analysis used to compute the amount of heat transferred across the annulus depends upon the flow regime. For the rarefied regime ($K_n > 1.0$) the equation for determining the heat flux per unit area is given by Reference 4 as:

$$\dot{q} = A_c \left(\frac{n+1}{n-1} \right) \sqrt{\frac{R}{8\pi}} \frac{P}{\sqrt{MT}} (T_2 - T_1) \quad (5)$$

For continuum flow regimes, the heat flux per unit area is given by Reference 5 as:

$$\dot{q} = -k \frac{(T_2 - T_1)}{(R_2 - R_1)} \quad (6)$$

An analysis was performed for the Apollo cryogenic storage tanks (Reference 6) assuming residual gas in the annulus consisted of air or the appropriate cryogen. Data shown in Table 3.3 are a result of this analysis and represent the heat conducted through the annulus by the residual gas. This heat transfer is in addition to the nominal heat flux to the tanks. The data shows that for an annulus pressure of less than approximately 10^{-7} psia, heat conduction by the residual gas is essentially negligible. However, heat conduction increases rapidly with increasing annulus pressure.

Table 3.4 summarizes the total heat transferred to the tanks as a function of the annulus pressure. Heat transfer calculations for annulus pressures of 15, 75, and 90 psia were carried out for continuum flow using Equation (6). Calculations for the remaining pressures shown in Tables 3.3 and 3.4 were performed for the rarefied regime using Equation (5).

The total heat transfer to the tanks as a function of the annulus pressure is shown in graphical form in Figures 3.3 and 3.4. These figures indicate that for annulus pressures greater than approximately 10^{-6} and 10^{-5} psia, respectively, for the oxygen and hydrogen tanks, the heat transfer increases significantly.

TABLE 3.3 RESIDUAL GAS CONDUCTION CALCULATIONS

$$\dot{q} = 4550 \sqrt{\frac{R}{M}} \frac{P}{\sqrt{T_g}} \cdot (T_2 - T_1) = \Lambda \frac{P}{\sqrt{T_g}}$$

CSS TANK TYPE	RESIDUAL GAS	ASSUMED $T_2 - T_1$ °R	$\sqrt{\frac{R}{M}}$	Λ *	ANNULUS PRESSURE (PSIA)	AVERAGE ANNULUS TEMPERATURE °R	RESIDUAL GAS CONDUCTION BTU/HR FT ²
OXYGEN	OXYGEN	220	6.98	6.98×10^6	2×10^{-5}	420	6.82
					1×10^{-5}	415	3.43
					1×10^{-6}	400	0.35
HYDROGEN	AIR	220	7.3	7.3×10^6	2×10^{-5}	420	7.13
					1×10^{-5}	415	3.58
					1×10^{-6}	400	0.365
	HYDROGEN	420	27.7	5.29×10^{-7}	2×10^{-5}	320	59.1
					1×10^{-5}	315	29.8
					1×10^{-6}	300	3.06
AIR	AIR	420	7.3	1.392×10^7	1×10^{-7}	272	0.231
					2×10^{-5}	320	15.58
					1×10^{-5}	315	7.85
					1×10^{-6}	300	.805
					1×10^{-7}	272	.0845

* Λ defined as, $\Lambda = 4550 \sqrt{\frac{R}{M}} (T_2 - T_1)$

TABLE 3.4 CSS TANK HEAT LEAK SUMMARY

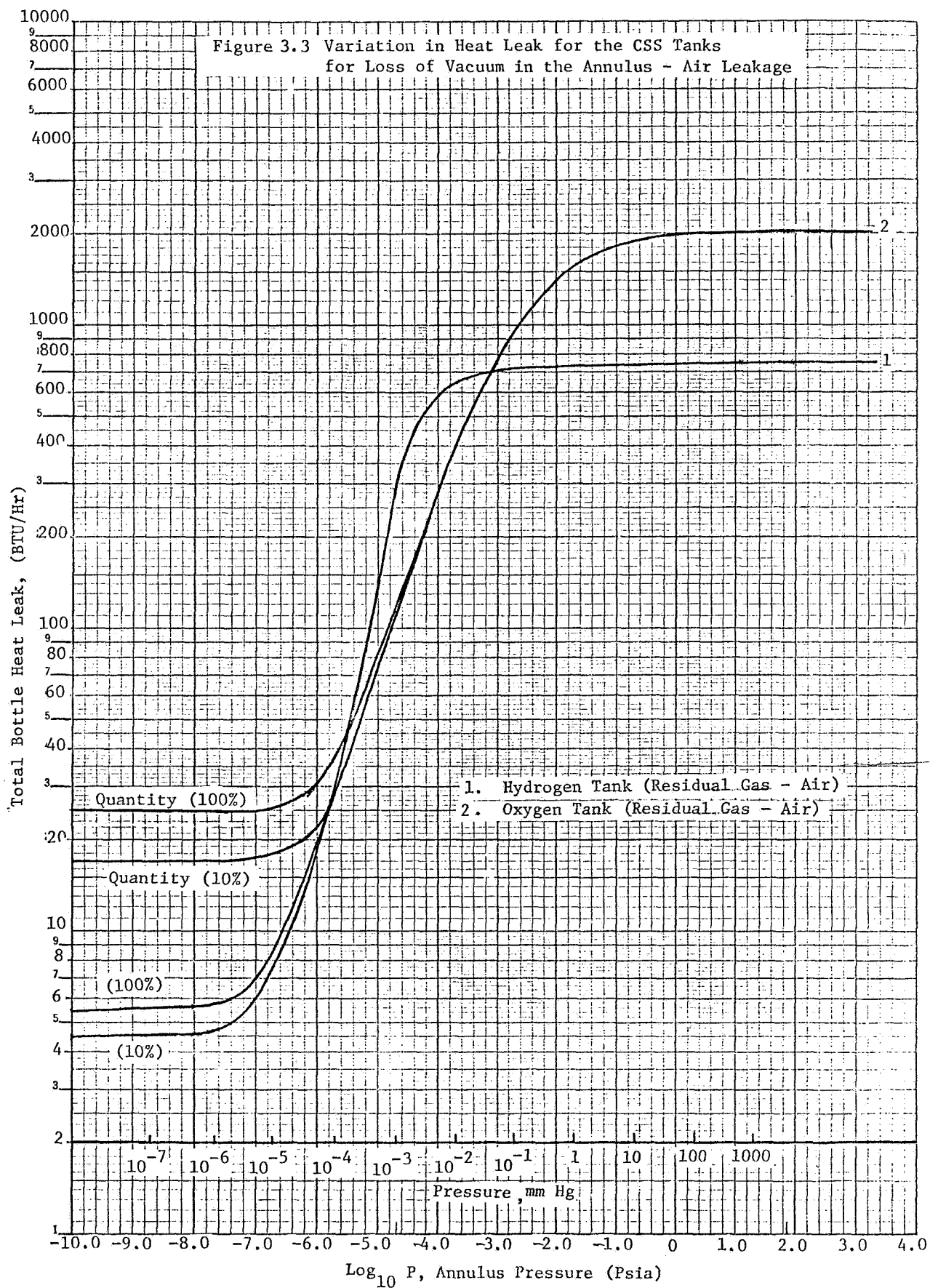
$$Q = \dot{q}A$$

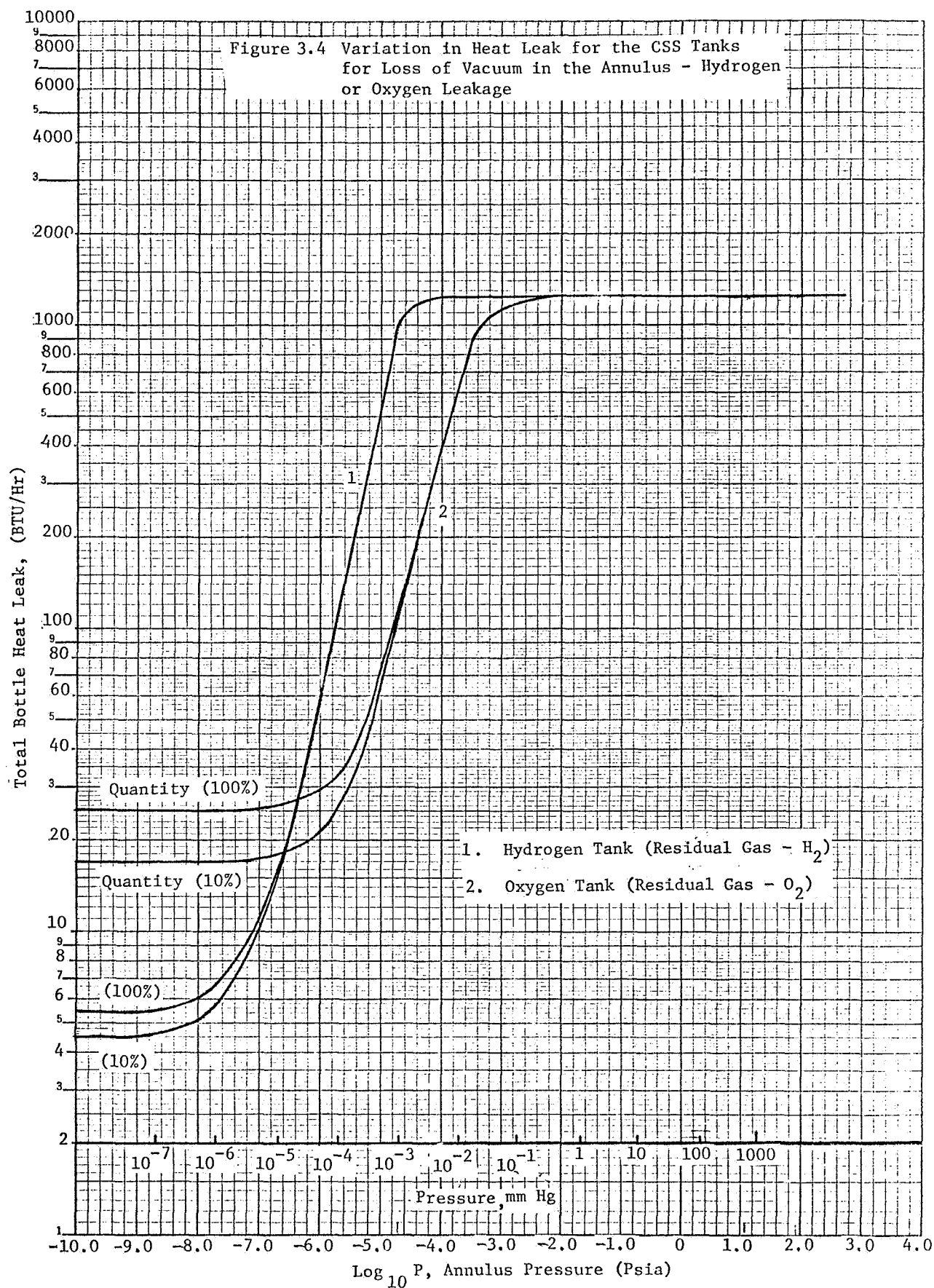
$$\text{where: } A_{O_2} = 13.7 \text{ ft}^2$$

$$A_{H_2} = 17.5 \text{ ft}^2$$

MODE & CURVE	PRESSURE		Log ₁₀ P PSIA	\dot{q} Cond. BTU/HR/FT ²	Q Cond. BTU/HR	Q _{H.L.} [*] Nom. \dot{W} BTU/HR		Q _T BTU/HR	
	PSIA	TORR (mm)				10% Full	100% Full	10% Full	100% Full
1. H ₂ Tank Air-Res. Gas	90.	4.6x10 ³	1.95	—	750.	4.5	5.5	755	755
	15.	7.6x10 ²	1.176	—	744.			749	749
	2. x 10 ⁻⁵	1x10 ⁻³	-4.70	15.58	272.	↑	↑	277	277
	1 x 10 ⁻⁵	5x10 ⁻⁴	-5.0	7.85	137.			142	142
	1 x 10 ⁻⁶	5x10 ⁻⁵	-6.0	.805	14.1			18.6	19.6
	1 x 10 ⁻⁷	5x10 ⁻⁶	-7.0	.0845	1.48			5.98	6.98
2. H ₂ Tank H ₂ Res. Gas	1 x 10 ⁻⁸	5x10 ⁻⁷	-8.0	.009	.15			4.7	5.7
	90.	4.6x10 ³	1.95	—	1250.			1255	1255
	15.	7.6x10 ²	1.176	—	1240.			1245	1245
	2. x 10 ⁻⁵	1x10 ⁻³	-4.70	59.1	1033.	↓	↓	1038	1038
	1 x 10 ⁻⁵	5x10 ⁻⁴	-5.0	29.8	521.			526	526
	1 x 10 ⁻⁶	5x10 ⁻⁵	-6.0	3.06	53.5			58	59
3. O ₂ Tank Air Res. Gas	1 x 10 ⁻⁷	5x10 ⁻⁶	-7.0	.321	5.62			10.12	11.12
	1 x 10 ⁻⁸	5x10 ⁻⁷	-8.0	.0338	.592	4.5	5.5	5.1	6.1
	75.	3.8x10 ³	1.875	—	2010.	17.0	25.0	2027	2035
	15.	7.6x10 ²	1.176	—	2000.	↑	↑	2017	2025
	2. x 10 ⁻⁵	1x10 ⁻³	-4.70	7.13	97.6			114.6	122.6
	1 x 10 ⁻⁵	5x10 ⁻⁴	-5.0	3.58	49.0			66.	84.
4. O ₂ Tank O ₂ Res. Gas	1 x 10 ⁻⁶	5x10 ⁻⁵	-6.0	.365	5.0			22.	30.
	1 x 10 ⁻⁷	5x10 ⁻⁶	-7.0	.04	.55			17.6	25.6
	75.	3.8x10 ³	1.875	—	1260.			1277	1285
	15.	7.6x10 ²	1.176	—	1250.			1267	1275
	2.0 x 10 ⁻⁵	1x10 ⁻³	-4.70	6.82	93.5	↓	↓	110.5	118.5
	1 x 10 ⁻⁵	5x10 ⁻⁴	-5.0	3.43	47.0			64.	72.
	1 x 10 ⁻⁶	5x10 ⁻⁵	-6.0	.350	4.8			21.8	29.8
	1 x 10 ⁻⁷	5x10 ⁻⁶	-7.0	.04	.55	17.0	25.0	17.6	25.6

* The nominal heat leak values were obtained from the CSS Flight Support Handbook (Reference 1), Figures 3.4.4 and 3.3.5 at flows of $\dot{m}_{O_2} = .88 \text{ lb/hr}$ and $\dot{m}_{H_2} = 0.10 \text{ lb/hr}$.





These curves have been incorporated into the storage tank thermal model. When the thermal subroutine encounters a failed tank flag, it uses the data presented in the figures to determine the heat flux to the tank based upon the vacuum jacket pressure. This pressure is an input to the program.

3.3 Components and Lines Model

The components and lines model is a two stage, transient and instantaneous steady state mathematical representation of the physical system. A lumped parameter explicit transient model (matrix model) is used to determine the proportioning of the flow rate from the tanks and the subsequent flow rate distribution in the lines. The matrix model includes the system from the storage tank to the point where the single line flow rate is uniquely determined by the EPS and/or ECS flow requirements and any leakage downstream of that point. Non-linear characteristics of the various components are accounted for in the solution by iteration of a characteristic matrix. The instantaneous steady state model (nodal model) is used to update the component characteristics in each iteration as well as to determine the thermodynamic properties for the entire system.

The specific configuration discussed in this document is for the Apollo 14 H-Mission. Subsequent configurations, to be included in the Integrated Systems Program will be modeled similarly in nature, but will differ in the plumbing and tankage arrangement.

3.3.1 Model Description

In order to achieve an efficient method of determining the flow distribution from the tanks, an explicit solution of an equivalent linear circuit is used as the first stage of the matrix model. The nonlinear characteristics are determined by the iteration of a characteristic matrix. This method of solution was chosen over a response vector iteration

technique because it assures a flow balance (conservation of mass) for each individual iteration as opposed to a near mass balance for the final iteration only. That is, the scheme chosen will enable a wider band convergence criteria than alternate methods. The linearization required for this type of solution was developed using the following electrical analogy.

The instantaneous pressure drop for incompressible flow across a line with inlet at station i and outlet at station j is given by:

$$\Delta P_{i-j} = \left(\frac{4fL}{D} \right)_{ij} \cdot \frac{\rho v^2}{2g_c} \quad (7)$$

Since

$$\dot{m} = \rho v A, \quad (8)$$

Equation (7) becomes

$$\Delta P_{i-j} = \left(\frac{4fL}{D} \right)_{ij} \cdot \frac{\dot{m}^2}{2g_c A^2} \quad (9)$$

Introducing a mean density between i and j as

$$\rho_{ij} = \frac{1}{R} \frac{P_i + P_j}{T_i + T_j}, \quad (10)$$

the following equation is obtained

$$P_i^2 - P_j^2 = \left[\frac{R}{2g_c A^2} (T_i + T_j) \left(\frac{4fL}{D} \right)_{ij} \right] \dot{m}^2 \quad (11)$$

Noting that for laminar flow in a cylindrical cross section

$$f = \frac{16}{N_{Re}} = \frac{4\pi\mu D}{\dot{m}}, \quad (12)$$

Equation (11) becomes

$$P_i^2 - P_j^2 = \frac{R}{2g_c A^2} (T_i + T_j) (16\pi\mu L) \dot{m} \quad (13)$$

setting

$$P^2 = E \quad (14)$$

and

$$\dot{m} = I \quad , \quad (15)$$

Equation (13) becomes

$$\Delta E = \frac{I}{G} \quad , \quad (16)$$

where

$$G = \left[\frac{R}{2g_c A^2} (T_i + T_j) (16\pi\mu L)_{ij} \right]^{-1} . \quad (17)$$

For a perfect gas

$$V_o \frac{d\rho}{dt} = \frac{V_o}{RT^2} \left[T \frac{dP}{dt} - P \frac{dT}{dt} \right] \quad (18)$$

Introducing Equation (14) into Equation (18) results in

$$V_o \frac{d\rho}{dt} = \frac{V_o}{2RT \sqrt{E}} \frac{dE}{dt} - \frac{V_o \sqrt{E}}{RT^2} \frac{dT}{dt} . \quad (19)$$

That is, in the transform variables

$$C \frac{dE}{dt} - I_R \approx V_o \frac{d\rho}{dt} \quad , \quad (20)$$

where C is an equivalent capacitance equal to

$$C = \frac{V_o}{2RTP} \quad , \quad (21)$$

and I_R is an equivalent residual current given by:

$$I_R = \frac{V_o P}{RT^2} \frac{dT}{dt} \quad (22)$$

Therefore, the transient flow circuit representation is given by:

$$V_o \frac{dp}{dt} = \sum \dot{m} \quad (23)$$

and has an equivalent electrical circuit representation equal to:

$$C \frac{dE}{dt} - I_R = \sum I \quad (24)$$

The overall flow diagram of the program is shown in Figure 3.5. Subsequent to initialization, the program evaluates the capacitance and residual current terms, and the conductances for the various legs required by the matrix mode. The conductances are initially evaluated from input resistor data and subsequently from resistor values calculated in the nodal component model. The matrix model evaluates the pressures at the various leg intersections from which the flowrates in the various legs are determined. The nodal component model processes the flow, pressure, and temperatures at each component and re-evaluates the component resistance values for resulting non-linearity. If only minor adjustments to the resistor values are required, the program proceeds to the next time step. Otherwise, the program returns to obtain a finer evaluation of the leg intersection pressures and flows.

3.3.2 Matrix Model

The matrix model is used to evaluate the pressure at the various flow line intersections as a function of tank conditions, and oxygen and hydrogen flow requirements. Separate models are used for the oxygen and hydrogen systems.

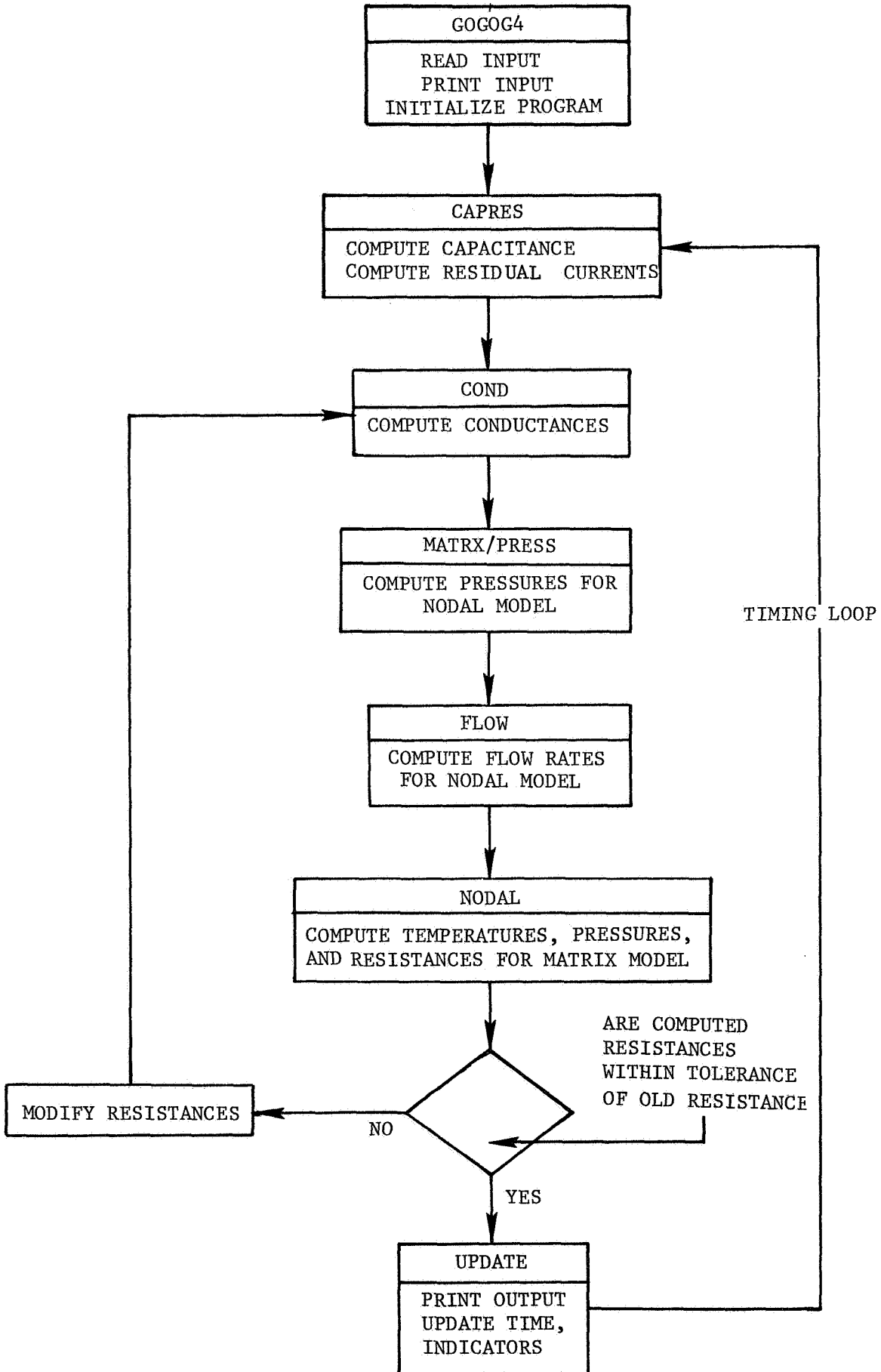


Figure 3.5
Components Line Model Flow Diagram

Schematics of the matrix models are shown in Figures A-1 and A-2 (Appendix III) for the oxygen and hydrogen systems. The models process a set of linear simultaneous equations for a finite time increment. The characteristic matrix has two floating columns and rows and the boundary condition vector has two floating columns. These additional elements are used to expand the system of equations to incorporate up to two leaks at arbitrary locations in each of the systems. For compressible flow such as leaks and overboard venting in which the flow is choked

$$\frac{\dot{m}_i \sqrt{T_i}}{P_i A_i} = K \quad . \quad (25)$$

This electrical equivalent is a short to ground given by

$$E = \frac{I}{G} \quad , \quad (26)$$

where

$$G = \frac{A_i K}{P_i \sqrt{T_i}} \quad . \quad (27)$$

Heating or cooling of the fluid in the lines due to an interchange of energy with the bay environment is modeled as a single pass heat exchanger with a constant sink temperature T_s over a given length. The relation is

$$\frac{T_j - T_i}{T_s - T_i} = 1 - e^{-UA/\dot{m}c_p} \quad (28)$$

or for direct incorporation into Equation (13)

$$T_j + T_i = T_s (1 - e^{-UA/\dot{m}c_p}) + T_i (1 + e^{-UA/\dot{m}c_p}) \quad (29)$$

Substituting Equation (29) into Equation (13) the pressure loss across a line segment becomes

$$P_i^2 - P_j^2 = \frac{R}{2g_c A^2} \left[T_s (1 - e^{-UA/\dot{m}c_p}) + T_i (1 + e^{-UA/\dot{m}c_p}) \right] 16\pi\mu L \dot{m} \quad (30)$$

where UA is a linearized radiant interchange factor given by

$$UA = \frac{\sigma}{8} \epsilon A (2T_s + T_j + T_i) (4T_s^2 + (T_i + T_s)^2) \quad (31)$$

Equation(30) is the final line pressure loss equation for compressible fluid flow and heat addition from the surrounding environment.

A typical lumped parameter equation used in representing the oxygen system is:

$$G_3(E_1 - E_2) = C_2 \frac{dE_2}{dt} + G_4(E_2 - E_4) + G_{10}(E_2 - E_{10}) - I_{R2}$$

where the subscripts refer to node location numbers and line legs. The hydrogen system lumped parameter equations are similar to the oxygen system equations. A complete list of the lumped parameter equations for both the oxygen and hydrogen systems is presented in Appendix III along with figures indicating node locations and tables presenting the line volumes used in the capacitance and residual current terms.

3.3.3 Nodal Model

The nodal components model processes the flow, pressure and temperature at each individual component. These components are analyzed as follows:

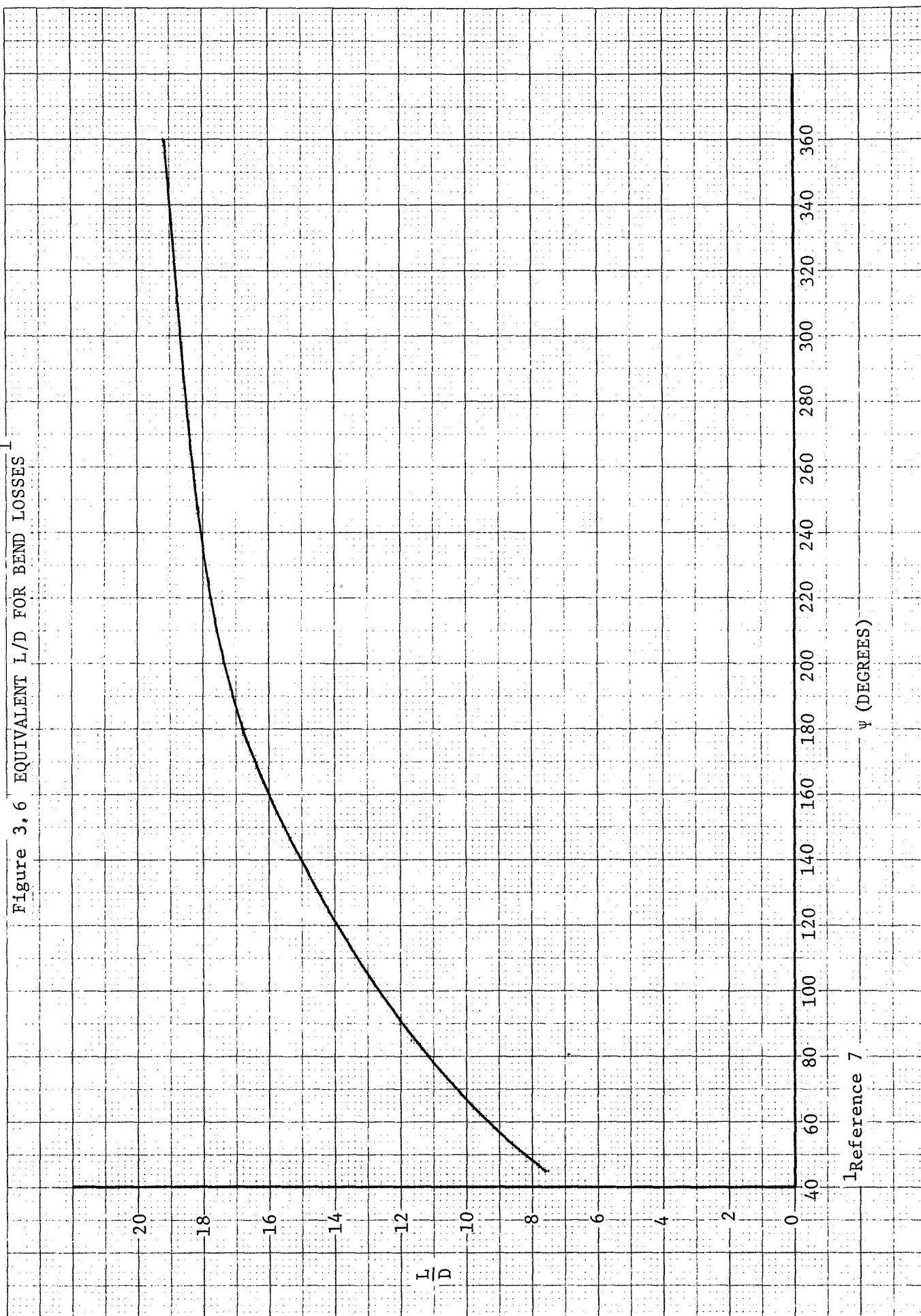
Lines and Fittings

The pressure loss in lines including fittings and bends from inlet i to outlet j is calculated by

$$P_i^2 - P_j^2 = \left[\frac{128\mu LR}{\pi g D_c^4} (T_i + T_j) \right] \dot{m} \quad (32)$$

where the temperatures are evaluated from Equations (30). Bend losses are incorporated by an equivalent L/D. The dependence of L/D to bend angle is shown in Figure 3.6. B-nuts and fittings are incorporated by an equivalent L/D of 3.0.

Figure 3.6 EQUIVALENT L/D FOR BEND LOSSES¹



Filters

The pressure loss across a filter is evaluated similar to the pressure losses computed for the lines and fittings except that due to the relatively short length the flow process is assumed adiabatic. That is, from inlet i to outlet j:

$$P_i^2 - P_j^2 = \left[\frac{256\mu LR}{\pi g_c D^4} T_i \right] \dot{m} \quad (33)$$

The equivalent L/D for filter is assumed to be 100.0.

Check Valves

The pressure loss across check valves is evaluated similar to that computed for filters where:

$$P_i^2 - P_j^2 = \left[\frac{256\mu LR}{\pi g_c D^4} T_i \right] \dot{m} \quad (34)$$

when the valve is open, and:

$$P_i^2 - P_j^2 = \frac{1}{G} \dot{m} \quad (35)$$

when the valve is closed.

The conductance term, G, used in Equation (35) is illustrated in Figure 3.7. Note that negative reseal and cracking pressures may be used to simulate back flow or internal leakage.

Relief Valves

Relief valves are evaluated in a manner similar to that used for evaluating the check valves where:

$$P_i^2 - P_j^2 = \left[\frac{256\mu LR}{\pi g_c D^4} T_i \right] \dot{m} \quad (36)$$

when the valve is open, and

$$P^2 - P_j^2 = \frac{1}{G} \dot{m} \quad (37)$$

when the valve is closed.

The conductance used in Equation (37) is presented in Figure 3.8.

Negative cracking and reseal pressures may be used to simulate check valve malfunction.

Shutoff Valve

The shutoff valve pressure loss is calculated similar to that of a filter. For this calculation the L/D ratio is set equal to 10 when the valve is opened and the conductance is set to 10^{-8} when the valve is closed.

Restrictors

The pressure drop across the flow restrictors is evaluated using the data shown in Figure 3.9.

Overboard Vents and Leaks

The effect of overboard vents and leaks on the system performance is evaluated assuming the flow through the leak or vent is sonic, and applying Equations (25) and (26).

A schematic of the nodal model network for the oxygen system is shown in Figure 3.10. Constants used in the system are given in Table 3.5. A schematic of the nodal model network for the hydrogen system is shown on Figure 3.11. Constants used in the system are given in Table 3.6.

FIGURE 3.7 CHECK VALVE RESISTANCE CHARACTERISTICS

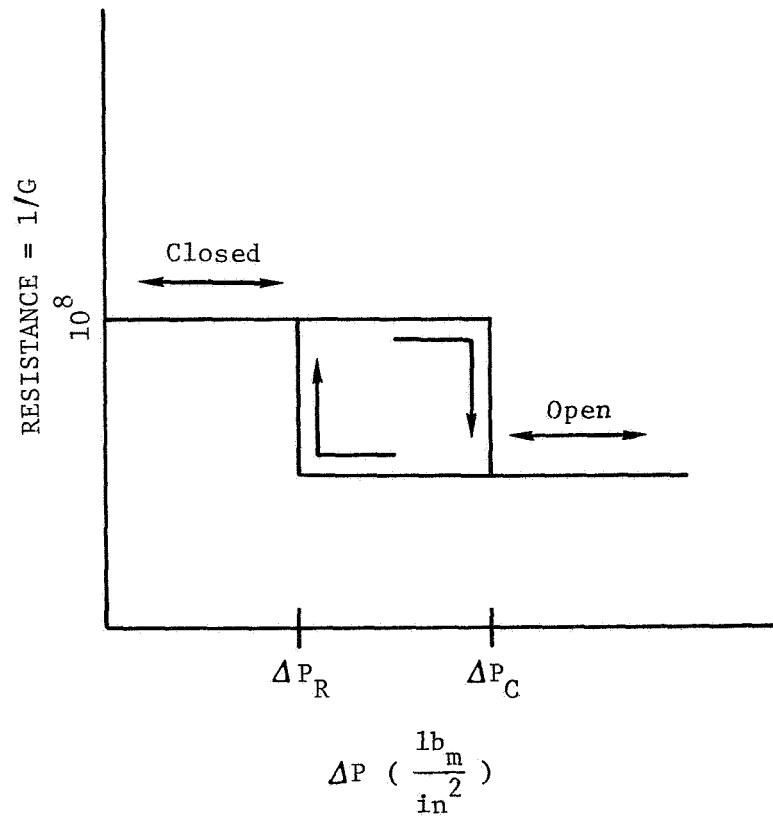


FIGURE 3.8 RELIEF VALVE RESISTANCE CHARACTERISTICS

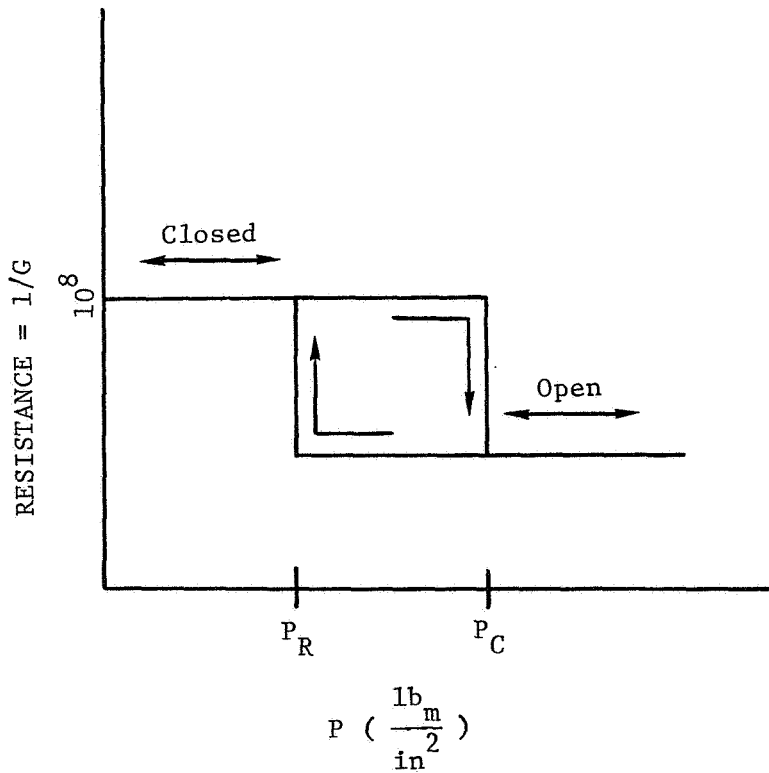
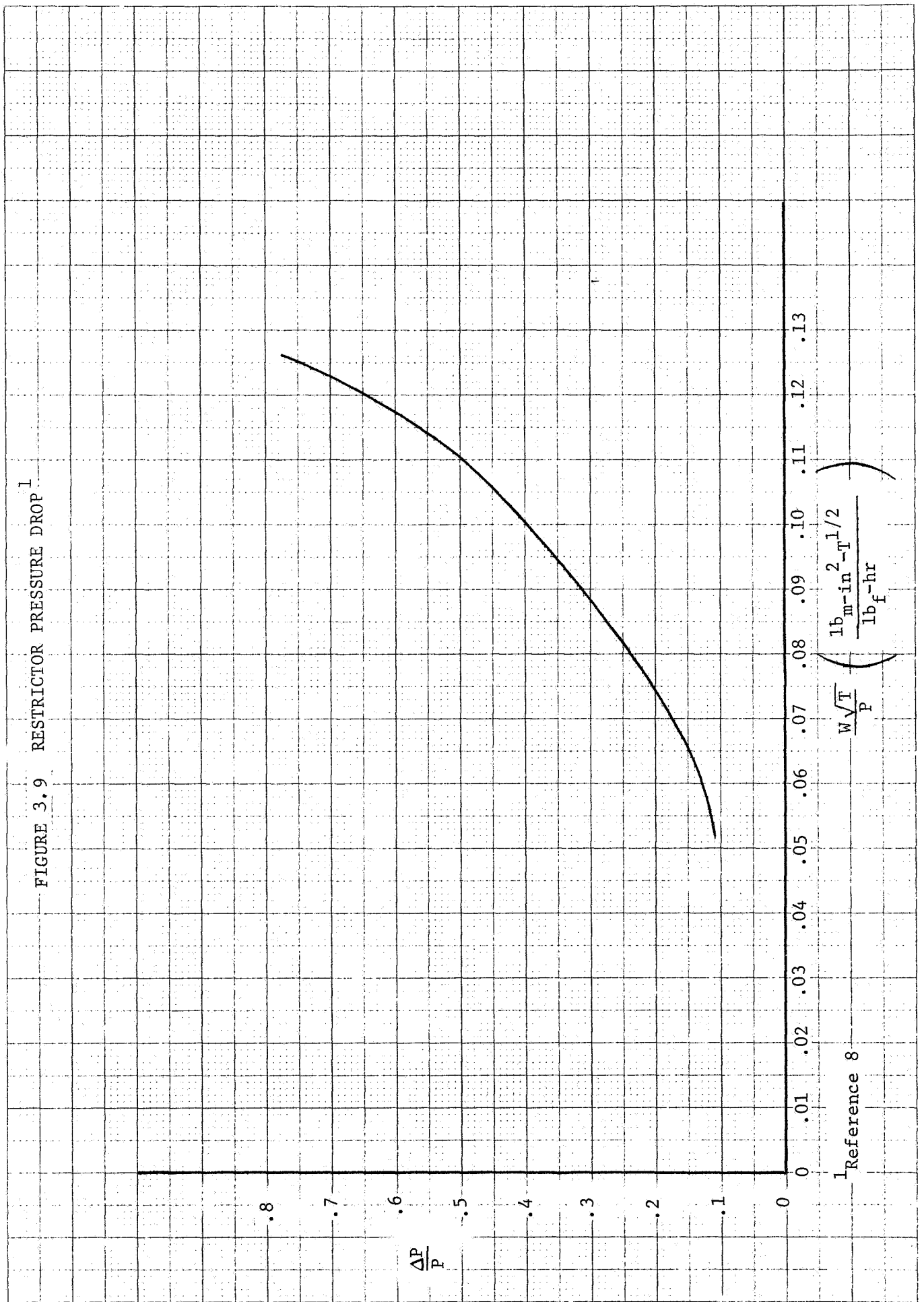




FIGURE 3.9 RESTRICTOR PRESSURE DROP¹



¹Reference 8



B	"B" Nut
C	Check Valve
F	Filter
L	Line
R	Relief Valve
RV	Relief Vent
U	Union
	Lumped Parameter
	Model
X	Purge Port

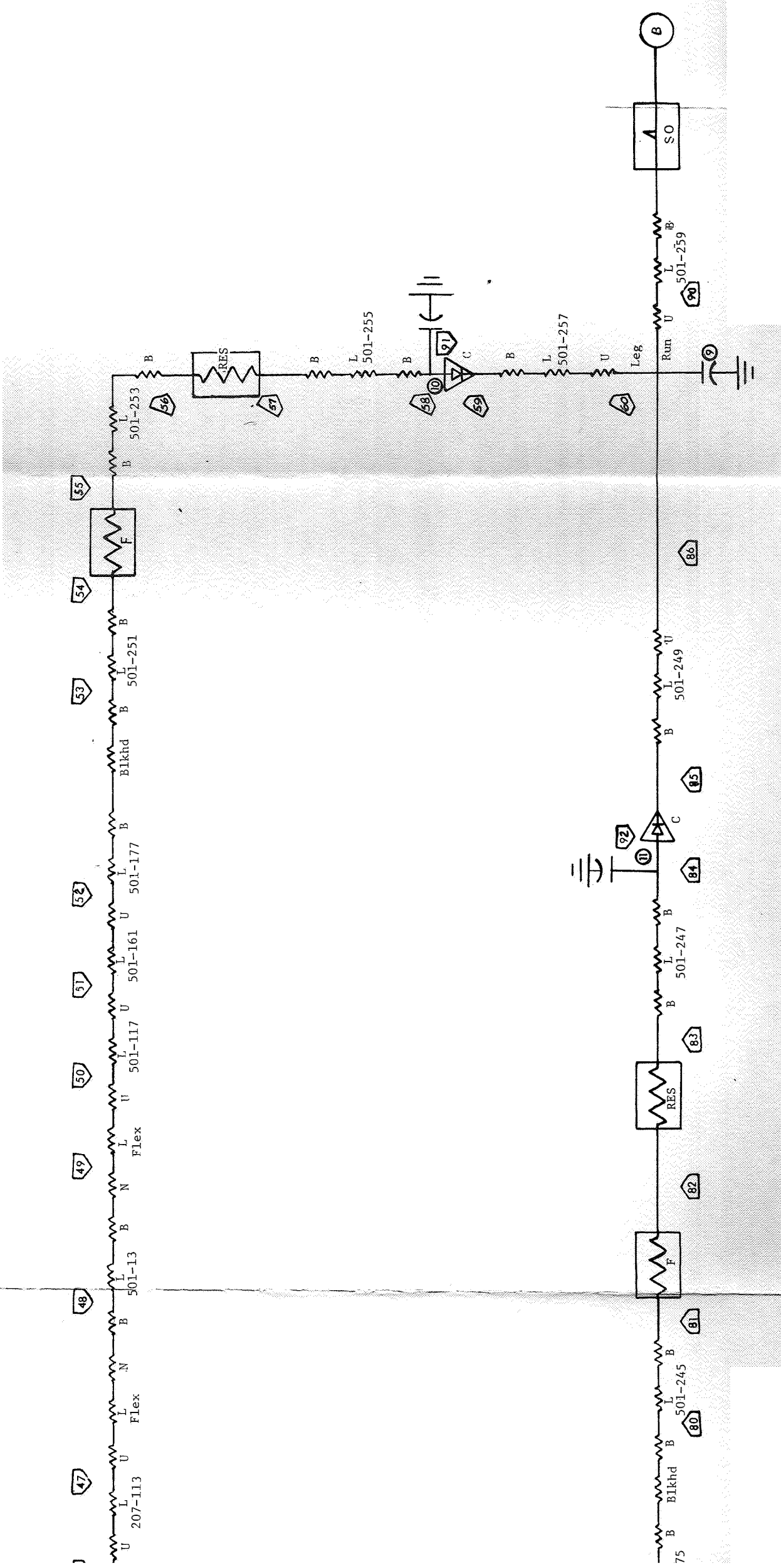


Table 3.5 Oxygen System Constants

LEG NO	NODE NO	L _{EFF} (IN)	D (IN)	A _{EFF} (IN ²)	P _c (LB _F /IN ²)	P _r (LB _F /IN ²)	SINK INDEX
1	1	10.50	0.21		999.	977.	
	2	63.54	0.21				163
	3			0.0346			
2	5	18.30	0.21				163
	6	21.00	0.21				
	7	42.26	0.21				163
	8						
3	10	74.65	0.21				163
	11	79.08					163
	12	89.50					150
	13	46.32					151
	14	21.00			3.	1.5	
	15	5.85	0.21				151
	16						
4	18	8.15	0.21				151
	19	18.62					151
	20	2.10					
	21	54.39					151
	22	40.06	0.21				151
	23						
5	24	42x10 ⁵	0.21		3.	1.5	
	25	32.11	0.21				151
	26						
6	27	10.50	0.21		999.	977.	
	28	16.62	0.21				151
	29						
7	30	36.62	0.21				151
	31	21.00	0.21				
	32	37.11	0.21				151
	33						

¹Data obtained or derived from system drawings and References 9 and 10.

Table 3.5 (Cont'd)

8	35	18.29	0.21			151
	36	21.00				
	37	43.39				151
	38	16×10^5	0.21	3.	1.5	
	39					
9	40	21.63	0.21			
	41	24.92	0.21			151
	42	16×10^5	0.21	3.	1.5	
	43					
10	44	80.25	0.21			152
	45	24.32				152
	46	78.03				153
	47	17.92				160
	48	64.49				160
	49	16.30	0.21			160
	50	81.66	0.18			161
	51	61.24				161
	52	29.26				161
	53	31.62	0.18			162
	54	21.00	0.21			
	55	20.32	0.21			162
	56					
	57	85.64	0.21			162
	58					
11	61	29.37	0.21			151
	62	21.00	0.21			
	63	39.06	0.21			151
	64					
12	65	18.71	0.21			151
	66					

Table 3.5 (Cont'd)

13	67	10.50	0.21	1000.5	977.	
	68	25.14	0.21			151
	69					
14	70	25.51	0.21			151
	71	86.01				152
	72	20.32				152
	73	77.62				153
	74	17.29				160
	75	56.21				160
	76	16.80	0.21			160
	77	82.91	0.18			161
	78	57.73	0.18			161
	79	34.73	0.18			161
	80	18.69	0.21			162
	81	21.00	0.21			
	82					
	83	5.35				162
	84					
15	87	43.94	0.338			151
	88			0.0897		
16	91	45×10^5	0.21	3.	1.5	
	59	2.76	0.21			162
	60					
17	92	42×10^5	0.21	3.	1.5	
	85	10.05	0.21			162
	86					

Figure 3.11
Model Model Network
H Mission Hydrogen System
Lines and Components

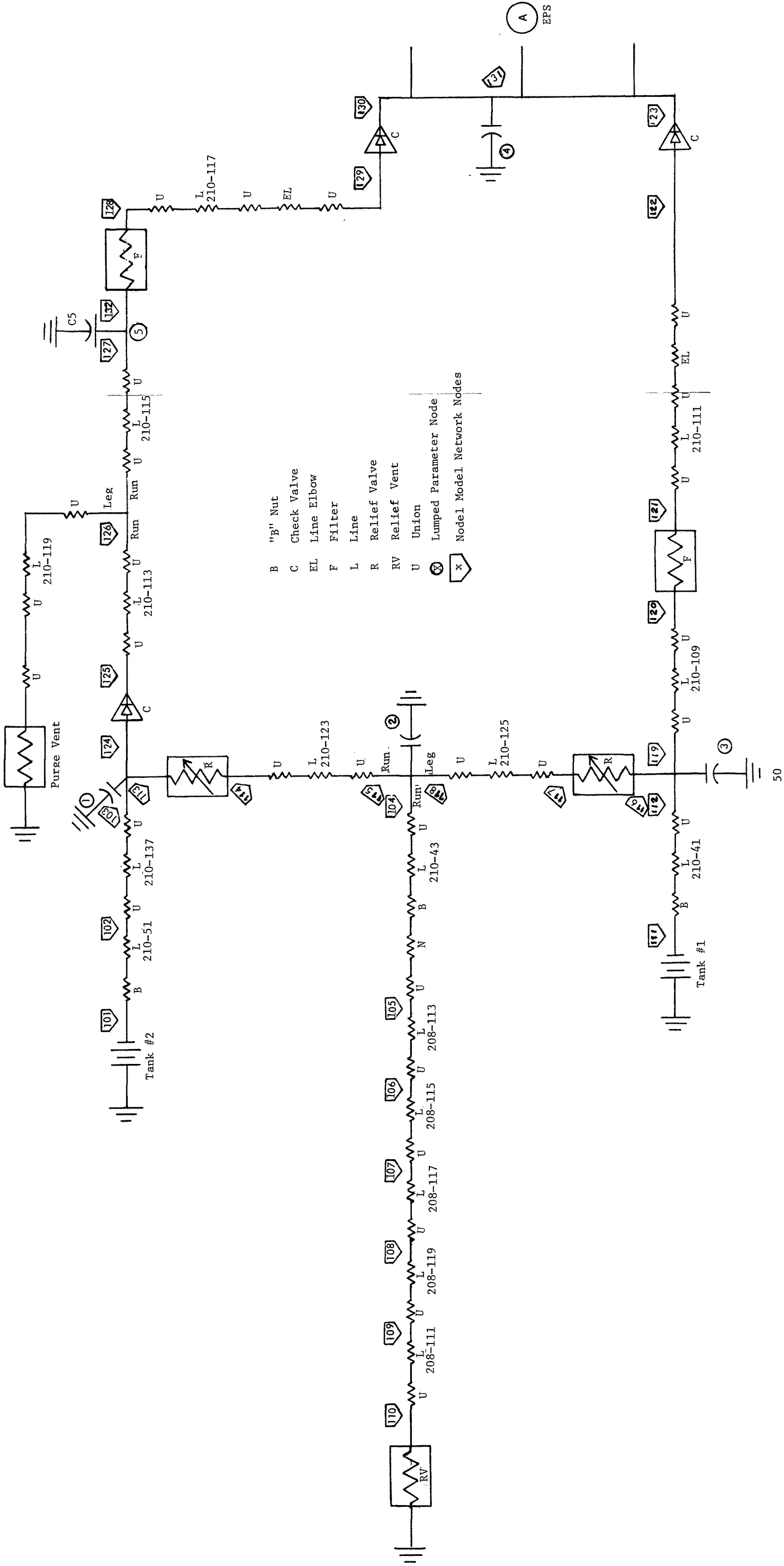


Table 3.6 Hydrogen System Constants ¹

LEG NO	NODE NO	L _{EFF} (IN)	D (IN)	A _{EFF} (IN ²)	1 P _c ⁽²⁾ (LB _F /IN ²)	P _r ⁽³⁾ (LB _F /IN ²)	SINK INDEX
1	101	40.67	0.21				154
	102	33.86	0.21				155
	103						
2	104	59.22	0.335				156
	105	84.70					156
	106	62.09					157
	107	39.60					152
	108	51.53					158
	109	174.10	0.335				159
	110			0.880			
3	111	61.86	0.21				155
	112						
4	113	10.50	0.21		281.5	273.5	
	114	23.28	0.21				155
	115						
5	116	10.50	0.21		280.	274.	
	117	16.76	0.21				155
	118						
6	119	23.14	0.21				155
	120	21.00					
	121	23.80					155
	122	126x10 ⁵	0.21		3.	1.5	
	123						
7	124	21.00	0.21		3.	1.5	
	125	33.14					155
	126	22.93					155
	127						
8	132	21.00					
	128	28.49					155
	129	126x10 ⁵	0.21		3.	1.5	
	130						

¹Data obtained or derived from systems drawings and References 9 and 10.

3.4 Thermophysical Properties for Oxygen and Hydrogen

Computer subroutines for computing the thermophysical properties for oxygen and hydrogen have been developed for inclusion into the Apollo Cryogenic Systems Programs. The majority of the data used in these subroutines has been recommended by the National Bureau of Standards (NBS). That data not available from the NBS was taken from Reference 11 (Stewart). In general, these subroutines determine pressure (P), temperature (T), density (ρ), enthalpy (H), the specific heat at constant pressure (c_p), the specific heat at constant volume (c_v), viscosity (μ), thermal conductivity (k), isotherm and isochor derivatives and the functions ϕ and θ , providing sufficient information concerning the fluid state is known. The data is included in the subroutines both in equation and table form. A routine is also included in the subroutines for interpolating between values from the tables.

3.4.1 Oxygen

Data contained in the subroutines for computing the thermophysical properties of oxygen were taken from References 11, 12 and 13. Reference 11 presents an equation of state for oxygen determined by R. B. Stewart. The isotherm and isochor derivatives were derived from this equation. While Reference 12 (Weber) also presents data for the isotherm and isochor derivatives, the results derived from Reference 11 are valid for a greater range. Both sets of data were included in the thermophysical subroutines to provide greater flexibility since the derivatives derived from Reference 11 may be determined with known values of temperature and density, while the data from Reference 12 requires that either pressure and temperature or pressure and density be given. Although the Weber data is preferred by NBS, the results using the equation developed by Stewart are quite acceptable for practical application.

The equation of state provided by Reference 11 may be used to compute pressure from known values of density and temperature. This equation is valid for temperatures between 117 and 540°R and for pressures to 5000 psia. The equation of state is as follows:

$$\begin{aligned}
 P = & \rho R T + (n_1 T + n_2 + n_3/T^2 + n_4/T^4 + n_5/T^6) \rho^2 \\
 & + (n_6 T^2 + n_7 T + n_8 + n_9/T + n_{10}/T^2) \rho^3 \\
 & + (n_{11} T + n_{12}) \rho^4 + (n_{13} + n_{14} T) \rho^5 \\
 & + \rho^3 (n_{15}/T^2 + n_{16}/T^3 + n_{17}/T^4) \exp(n_{25} \rho^2) \\
 & + \rho^5 (n_{18}/T^2 + n_{19}/T^3 + n_{20}/T^4) \exp(n_{25} \rho^2) \\
 & + \rho^7 (n_{21}/T^2 + n_{22}/T^3 + n_{23}/T^4) \exp(n_{25} \rho^2) \\
 & + n_{24} \rho^{(n_{28}+1)} \left(\rho^{n_{28}} - \rho_c^{n_{28}} \right) \exp \left[n_{26} \left(\rho^{n_{28}} - \rho_c^{n_{28}} \right)^2 + n_{27} (T - T_c)^2 \right] \quad (38)
 \end{aligned}$$

where: $\rho_c = 13.333$ gmol/liter, critical density

$T_c = 154.77$ °K, critical temperature

In this expression, P is in atmospheres, T is in °K, and ρ is in gmol/liter.

The constants for this equation are given in Table 3.7.

Equation (38) is programmed in Subroutine ØDTP. The subroutine converts the units of density from lbm/cu-ft to gmol/liter and temperature from °R to °K prior to use. The output pressure is in psia.

The isotherm derivative, $\left. \frac{\partial P}{\partial \rho} \right|_T$, is the partial derivative of Equation (38), with respect to the density at constant temperature, and is given by:

$$\left. \frac{\partial P}{\partial \rho} \right|_T = R T + \sum_{i=1}^{24} n_i X_i \quad (39)$$

Values for the variables in this equation are presented in Table 3.8.

TABLE 3.7
CONSTANTS FOR STEWART'S EQUATION OF STATE

$R = 0.0820535$	$n_{10} = -3.59419602 \times 10$	$n_{19} = -2.67817667 \times 10^2$
$n_1 = 3.38759078 \times 10^{-3}$	$n_{11} = 1.02209557 \times 10^{-6}$	$n_{20} = 1.05670904 \times 10^5$
$n_2 = -1.31606223$	$n_{12} = 1.90454505 \times 10^{-4}$	$n_{21} = 5.63771075 \times 10^{-3}$
$n_3 = 1.92049067 \times 10^3$	$n_{13} = 1.21708394 \times 10^{-5}$	$n_{22} = -1.12012813$
$n_4 = 1.92049067 \times 10^7$	$n_{14} = 2.44255945 \times 10^{-3}$	$n_{23} = 1.46829491 \times 10^2$
$n_5 = -2.90260005 \times 10^{10}$	$n_{15} = 1.73655508 \times 10^2$	$n_{24} = 9.98868924 \times 10^{-4}$
$n_6 = -5.70101162 \times 10^{-8}$	$n_{16} = 3.01752841 \times 10^5$	$n_{25} = -0.00560$
$n_7 = 7.96822375 \times 10^{-5}$	$n_{17} = -3.49528517 \times 10^7$	$n_{26} = -0.157$
$n_8 = 6.07022502 \times 10^{-3}$	$n_{18} = 8.86724004 \times 10^{-1}$	$n_{27} = -0.350$
$n_9 = -2.71019658$		$n_{28} = 0.90$

TABLE 3. 8 - VARIABLES FOR COMPUTING ISOTHERM DERIVATIVES

$X_1 = 2\rho T$	$X_9 = 3\rho^2/T$	$X_{17} = f_6/T^4$
$X_2 = 2\rho$	$X_{10} = 3\rho^2/T^2$	$X_{18} = f_7/T^2$
$X_3 = 2\rho/T^2$	$X_{11} = 4\rho^3/T$	$X_{19} = f_7/T^3$
$X_4 = 2\rho/T^4$	$X_{12} = 4\rho^3$	$X_{20} = f_7/T^4$
$X_5 = 2\rho/T^6$	$X_{13} = 5\rho^4$	$X_{21} = f_8/T^2$
$X_6 = 3\rho^2/T^2$	$X_{14} = 5\rho^4/T$	$X_{22} = f_8/T^3$
$X_7 = 3\rho^2/T$	$X_{15} = f_6/T^2$	$X_{23} = f_8/T^4$
$X_8 = 3\rho^2$	$X_{16} = f_6/T^3$	$X_{24} = f_9 f_2 f_3 + \rho^{(n_{28}+1)} f_{10} f_3 + \rho^{(n_{28}+1)} f_2 f_{11}$
$f_1 = \exp (n_{25} \rho^2)$		$f_6 = 3f_1 \rho^2 + f_5 \rho^3$
$f_2 = \rho^{n_{28}} - \rho^{n_{28}} c_2$		$f_7 = 5f_1 \rho^4 + f_5 \rho^5$
$F_3 = \exp [n_{26} f_2 + n_{27} (T-T_c)^2]$		$f_8 = 7f_1 \rho^6 + f_5 \rho^7$
$f_4 = 2n_{27} (T-T_c) f_3$		$f_9 = (n_{28}+1) \rho^{n_{28}}$
$f_5 = 2f_1 \rho^{n_{25}}$		$f_{10} = n_{28} \rho^{(n_{28}-1)}$
		$f_{11} = 2f_2 n_{26} f_3 f_{10}$

The coefficients n_i are the same as that for Equation (38). The subroutine for computing the isotherm derivative is ØDTIT. This subroutine converts density from lbm/cu-ft to g.mol/liter and temperature from °R to °K prior to its use in Equation (39). The output derivative is in units of psia-ft³/lbm.

The isochor derivative, $\left. \frac{\partial P}{\partial T} \right|_{\rho}$, is the partial derivative of Equation (38), with respect to temperature at constant density and is given by:

$$\left. \frac{\partial P}{\partial T} \right|_{\rho} = \rho R + \sum_{i=1}^{24} n_i X_i \quad (40)$$

where the n_i are the same as those listed for Equation (38). The variables in this equation are shown in Table 3.9.

The subroutine call for computing $\left. \frac{\partial P}{\partial T} \right|_{\rho}$ is ØDTIC. The procedure for conversion from one set of units to the other is the same as for Equations (38) and (39). The output derivative is in units of psia/°R.

In addition to providing data for the isotherm derivative and the isochor derivative, Reference 12, included data for density, enthalpy, specific heats (at constant pressure and volume) and the functions θ and ϕ . All are in tabular form. Further flexibility was provided by permitting these properties to be determined from known values of pressure and temperature or from pressure and density. These tables are valid for temperatures from 100 to 540°R at 5 degree increments and for pressures ranging from 588 to 1029 psia at increments of 73.5 psi. Table 3.10 lists the subroutines for determining each of the thermophysical parameters. In these subroutines, pressure is in psia, temperature is in °R and density is in lbm/ft³.

Data from Reference 13 is also in the form of tables and provides viscosity and thermal conductivity as functions of pressure and temperature. This data is valid for temperatures ranging from 180 to 540°R at increments

TABLE 3.9
VARIABLES FOR COMPUTING ISOCHOR DERIVATIVE

$X_1 = \rho^2$	$X_9 = -\rho^3/T^2$	$X_{17} = -4\rho f_1/T^5$
$X_2 = 0$	$X_{10} = -2\rho^3/T^3$	$X_{18} = -2\rho^5 f_1/T^3$
$X_3 = -2\rho^2/T^3$	$X_{11} = \rho^4$	$X_{19} = -3\rho^5$
$X_4 = -4\rho^2/T^5$	$X_{12} = 0$	$X_{20} = -4\rho^5 f_1/T^5$
$X_5 = -6\rho^2/T^7$	$X_{13} = 0$	$X_{21} = -2\rho^7 f_1/T^3$
$X_6 = 2T\rho^3$	$X_{14} = -\rho^5/T^2$	$X_{22} = -3\rho^7 f_1/T^4$
$X_7 = \rho^3$	$X_{15} = -2\rho^3 f_1/T^3$	$X_{23} = -4\rho^7 f_1/T^5$
$X_8 = 0$	$X_{15} = -3\rho^3 f_1/T^4$	$X_{24} = \rho^{(n_{28}+1)} f_2 f_4$
where: $f_1 = \exp(n_{28}\rho^2)$		
$f_2 = \rho^{n_{28}} - \rho_c^{n_{28}}$		

of 18 degrees and for pressures from 588 to 1029 psia at increments of 73.5 psi. The subroutines for determining these parameters are listed in Table 3.10.

3.4.2 Hydrogen

The thermophysical properties used in the hydrogen subroutine are based upon computer programs developed by the NBS (Reference 14). These properties are valid for pressures from 1 to 5000 psia and for temperatures ranging from 25 to 5000 °R (enthalpy from -130 to 20,000 BTU/lb). In the NBS programs all thermophysical properties are determined from known values of pressure and temperature and include enthalpy, density, specific heats for both constant pressure and constant volume, viscosity and thermal conductivity. However, in the subroutine developed for the Apollo Cryogenic System Programs, provision has been made to compute the pressure and temperature from other known properties. The pressure, density and temperature are in units of psia, lbm/ft³, and °R, respectively.

Pressure, psia

The NBS program expresses hydrogen density as a polynomial equation in terms of pressure and temperature, $\rho = \rho(P,T)$. In the subroutine HPDIT (ρ, T, P_A), pressure is determined from this equation as a function of density and temperature using a Newton-Raphson iteration method. P_A is an a priori value of pressure required to initiate the iteration and should be estimated as closely as possible to the actual value.

Temperature, °R

Temperature is computed in a manner similar to that of pressure as a function of the pressure and density. The subroutine call is HPDIT (P, ρ, T_A) where T_A is the a priori value of temperature required to initiate the iteration.

Table 3.10 lists the subroutines for determining the above properties as well as other parameters.

TABLE 3.10
THERMOPHYSICAL PROPERTIES SUBROUTINES

PROPERTY	UNITS	INPUT VARIABLE	SUBROUTINE NAME	REFERENCE
OXYGEN				
Density	lbm/ft ³	P&T	QPTD	12
Enthalpy	btu/lbm	P&T	QPTH	12
Enthalpy	btu/lbm	P&ρ	QPDH	12
Function θ	btu/lbm	P&T	QPTPT	12
Function φ	psia-ft ³ /btu	P&T	QPTPT	12
Isochor	psia/°R	T&ρ	QDTIC	11
Isochor	psia/°R	P&T	QPTIC	12
Isochor	psia/°R	P&ρ	QPDIC	12
Isotherm	psia-ft ³ /btu	T&ρ	QDTIT	11
Isotherm	psia-ft ³ /btu	P&T	QPTIT	12
Isotherm	psia-ft ³ /btu	P&ρ	QPDIT	12
Pressure	Psia	T&ρ	QDTP	11
Specific Heat, C _p	°R/lbm	P&T	QPTCP	12
Specific Heat, C _p	°R/lbm	P&ρ	QPDCP	12
Specific Heat, C _v	°R/lbm	P&T	QPTCV	12
Specific Heat, C _v	°R/lbm	P&ρ	QPDCV	12
Thermal Conduc- tivity	btu(ft/hr)/ ft ² /°R	P&T	QPTTC	13
Temperature	°R	P&ρ	QPDT	12
Viscosity	lbf-hr/ft ²	P&T	QPTV	13
HYDROGEN				
Density	lbm/ft ³	P&T	HPID	14
Enthalpy	btu/lbm	P&T	HPTH	14
Function θ	btu/lbm	P&T	HPTPT	14
Function φ	psia-ft ³ /btu	P&T	HPTPT	14
Isochor	psia/°R	P&T	HPTPT	14
Isotherm	psia ft ³ /btu	P&T	HPTPT	14
Pressure	Psia	T&ρ	HPDIT	14
Specific Heat, C _p	°R/lbm	P&T	HPTCP	14
Specific Heat, C _p	°R/lbm	P&T	HPTCV	14
Specific Heat, C _v	°R/lbm	P&T	HPTCV	14
Thermal Conduc- tivity	btu(ft/hr)/ ft ² /°R	P&T	HPTTC	14
Temperature	°R	P&ρ	HPDIT	14
Viscosity	lbf-hr/ft ²	P&T	HPTV	14

4.0 PROGRAM RESTRICTIONS

The EQTANK Program is comprised of quasi-static equilibrium thermodynamic relations. Because of this, there are certain considerations that should be taken into account when using the program results. First, the total energy added to the fluid in a tank predicted by the EQTANK program may be higher than in actual practice because under actual conditions the colder fluid will be expelled, while the EQTANK model assumes that uniformly heated fluid is expelled. This leads to an overestimate of the amount of electrical power necessary to operate the CSS heaters and fans. Heater "on" times and cycle times predicted by the EQTANK program will also be longer than those experienced in flight due to the effects of stratification. In addition, the results of the EQTANK program will not resolve the change in pressurization decay rates from immediately after to immediately prior to tank heater energization.

The deviations described above are problems of resolution rather than of overall performance analysis deviations and do not limit the usefulness of the program. However, these restrictions should be accounted for in interpreting the program results.

Under high oxygen flowrate requirements, such as during extravehicular activity, turbulent flow may develop in the CSS lines or components. Although subroutines for both turbulent and laminar flow pressure loss evaluation are present in the PLMBNG program, the current version assumes laminar flow for all conditions. When incorporated into the Integrated Systems Program, the PLMBNG model will be capable of evaluating the flow regime and will compute the resulting pressure loss accordingly.

Currently, it is assumed that fluid leaving the CSS tanks reaches approximately ambient temperatures very rapidly. It was therefore assumed that the fluid could be considered a perfect gas. However, if simulations indicate that this assumption is unwarranted, a compressibility factor may be included to better simulate the real fluid. This factor may be obtained from the Thermophysical Properties Subroutine.

5.0 RECOMMENDATIONS

It is recommended that effort be directed toward determining model accuracy by operating the program for flight conditions and comparing the results with flight data.

It is recommend that the subroutine for predicting the potential pressure collapse as a function of flowrate, tank quantity and acceleration level be extracted from the EQTANK program and put into a form suitable for use during a flight.

It is further recommended that a simplified model be developed to determine the effects of stratification on heater cycling for incorporation into the CSS Integrated Simulation Program. This model would be in addition to the current model which approximates potential collapse pressure. A necessary step to the model development is the determination of the volume and density of an effective hot gas bubble next to the heater from flight data. The hot gas bubble determines the pressure in the tank and, thus, controls the heater cycle time. The method to accomplish this has been formulated. This model could be completed using Apollo 14 flight data.

6.0 REFERENCES

1. NASA Document, "Apollo Fuel Cell and Cryogenic Gas Storage System Flight Support Handbook," Manned Spacecraft Center, Houston, Texas, 18 February 1970.
2. Results of Detailed Stratification Analysis, obtained informally from C. K. Forestor, Boeing Co., Seattle, Washington.
3. Analysis of Oxygen Tank Heat Leak, obtained informally from Beech Aircraft Co., Boulder, Colorado.
4. Corruccini, R. J., "Gaseous Heat Conduction at Low Pressures and Temperatures", Vacuum, Vol. VII and VIII, April, 1959.
5. McAdams, W. H., "Heat Transmission", McGraw-Hill Book Company, 3rd Edition, 1954.
6. TRW IOC 70.4354.3-104, "Effect of CSS Tank Vacuum Annulus Leakage on Heat Transfer Rates," P. J. Knowles, 23 November 1970.
7. "Aerospace Applied Thermodynamics Manual," Aerospace Environmental Control Systems, February 1960.
8. NASA Document SNA-8-D-027(1), "CSM/LM Spacecraft Operational Data Book, Vol. 1," Manned Spacecraft Center, 15 April 1970.
9. "Flow of Fluids Through Valves, Fittings, and Pipes," Engineering Division, Crane Co., 1969.
10. Apollo 14 CSS End Item Acceptance Test Data.
11. Stewart, R. B., "The Thermodynamic Properties of Oxygen", PhD Thesis, University of Iowa, June, 1966.
12. Weber, L. A., "Thermodynamic and Related Properties of Oxygen from the Triple Point to 300°K at Pressures to 330 Atmospheres," NBS Report 9710A, 29 August 1968.
13. Roder, H. M., "Viscosity and Thermal Conductivity of Oxygen," NBS letter 275.02 to J. Smithson, EP5, NASA/MSC, September 24, 1970.
14. Hall, W. J., R. D. McCarty, and H. M. Roder, "Computer Programs for Thermodynamic and Transport Properties of Hydrogen," NBS Report #9288, (NASA - CR88086) , August, 1967.

APPENDIX I NOMENCLATURE

A	Area, in ² .
A _B	Surface area of the inner tank, ft ² .
A _c	Accommodation coefficient, equal to 1.0.
ACCELN(I,J)	Logarithm (base 10) of the acceleration magnitude in earth gravities, dimensionless.
C	Capacitance analog, $C = \frac{V_o}{2RTP}$, lbm-in ⁴ /lbf ²
c _p	Specific heat of fluid at constant pressure, btu/(lbm-°R).
c _v	Specific heat of fluid at constant volume, btu/(lbm - °R).
CYTIME(I,J)	Length of heater cycle, min.
D	Line diameter, in.
DPCDT	Total derivative of potential collapse pressure with respect to time, psia/hr.
DPDT(I,J)	Tank pressure rise or decay rate, psia/hr.
DPDTD	Dummy tank pressure rise rate, psia/hr.
DTG(I,J)	Time for tank pressure to change x psia, hr.
E	Electrical potential analog, $E = P^2$, lbf ² /in ⁴ .
f	Friction factor, dimensionless.
FTANK(I,J)	Tank flowrate, lb/hr.
G	Conductance analog lbf ² -hr/(lbm-in ⁴)
g _c	Gravity constant lbm-in/(lbf-hr ²)
HPV	Enthalpy of stored fluid, btu/lbm
HTON(I,J)	Heater on time, min.
HVCS	Enthalpy of fluid in vapor cooled shroud, btu/lbm.
I	Current analog, $I = \dot{m}$, lbm/hr.
I _R	Residual current analog, $I_R = \frac{PV_o}{RT^2} = \frac{dT}{dt}$, lbm/hr.

IFAND	Dummy pressure control switch flag for fan, dimensionless.
IFAN(I,J)	Pressure control switch flag for fan, dimensionless.
IHTRC(I,J)	Heater cycle counter, dimensionless.
IHTRD	Dummy pressure control switch flag for heater, dimensionless.
IPS(I,J)	Pressure control switch flag for each tank, dimensionless.
ISFD	Dummy fan control switch flag, dimensionless.
ISHD	Dummy heater control switch flag, dimensionless.
k	Thermal conductivity, btu/(hr-ft-°R).
K	Constant, $K = \left(\frac{g_c n}{R}\right)^{\frac{1}{2}} \left(\frac{n+1}{2}\right)^{-\frac{n+1}{2(n-1)}}$, lbm-°R ^{1/2} /(lbf-hr).
K_n	Knudsen number, λ/l , dimensionless.
l	Characteristic length, ft.
L	Length, in.
M	Gas molecular weight, lbm/(lb-mole)
\dot{m}	Mass flowrate, lbm/hr.
n	Ratio of specific heats, c_p/c_v , dimensionless.
N	Polytropic exponent for gas lines attached to tank, dimensionless.
N_{RE}	Reynolds number, $\frac{\rho V_o D}{\mu}$, dimensionless.
P,p	Pressure, psia
P_c	Collapse pressure, psia
PBAR	Average tank pressure over time interval, TCALC, psia.
PC(I,J)	Potential collapse pressure, psia.
PCT	Percentage of cryogen in tank, percent.
PHID	Dummy tank thermodynamic property, ft ³ -psia/btu.
PHI(I,J)	Tank thermodynamic property ϕ , ft ³ -psia/btu.
PNEXT	Pressure at which pressure switch will change position, psia.
PPPR	Partial of pressure with respect to density, ft ³ -°R/lbm.

PPPT	Partial of pressure with respect to temperature, psia/ ^o R.
PRCNT(I,J)	Usable fluid remaining in tank, percent.
PTPP(I,J)	Partial of temperature with respect to pressure, ^o R/psia.
PTPRO	Partial of temperature with respect to density, ^o R-ft ³ /lbm.
q	Total heat input rate, btu/hr.
\dot{q}	Heat leak flux, btu/(hr-ft ²)
Q	Heat leak, btu/hr.
Q(I,J)	Total tank heat input, btu/hr.
QLEAK(I,J)	Tank heat leak, btu/hr.
QR	Radiation heat leak, btu/hr.
r	Mean pressure vessel radius, in.
R	Universal gas constant.
R ₁	Inner tank wall radius, ft.
R ₂	Outer tank wall radius, ft.
RHOBAR	Average tank density over time interval, TCALC, lbm/ft ³ .
RHO(I,J)	Tank fluid density, lbm/ft ³ .
t	Time, hr.
T	Temperature, ^o R.
TBAR	Average tank temperature over time interval, TCALC, ^o R.
TCALC	Time interval chosen for updating all CSS tanks, hr.
TEXTIT(I)	Temperature of oxygen leaving vapor cooled shroud, ^o R.
THETAD	Dummy tank specific heat input, btu/lbm.
THETA(I,J)	Tank specific heat input, btu/lbm.
TLIMIT(I,J)	Time for tank pressure to reach pressure switch limit, hr.
TOS,T ₁	Temperature of tank outer wall, ^o R.
TPV,T ₂	Temperature of tank outer wall, ^o R.
TVCS	Average temperature of fluid in vapor cooled shroud, ^o R.

u	Internal energy of fluid, btu/lbm.
U	Overall heat transfer coefficient, btu/(hr-in ² -°R).
v	Fluid velocity, in/hr.
V	Tank Volume, ft ³ .
V_o	Tank Volume, in ³ .
V_2	Volume of lines attached to tank, ft ³ .
$WT(I,J)$	Weight of fluid in tank, lbm.
Y	Young's modulus for tank material, psi.
α	Tank material thermal expansion coefficient, 1/°R.
β	Tank thickness, in.
$\frac{\partial P}{\partial t}$	Time rate of change of pressure, psia/hr.
$\frac{\partial T}{\partial \rho_o}$	Isobaric derivative for fluid, °R-ft ³ /lbm.
$\frac{\partial T}{\partial P}$	Isochor derivative for fluid, °R/psia.
Δ	Difference, dimensionless
ϵ	Emissivity, dimensionless
θ	Thermodynamic function, $-\rho_o \frac{\partial H}{\partial \rho_o} \bigg _P$, btu/lbm.
λ	Mean free path, ft.
Λ	$4550 \frac{R}{M} (T_2 - T_1)$.
μ	Viscosity, lbm/(in-hr).
ρ	Fluid density, lbm/in ³ .
ρ_o	Fluid density, lbm/ft ³ .
σ	Stephan-Boltzman constant, $\sigma = 1.1 \times 10^{-11}$, btu/(hr-in ² -°R ⁴).

ν	Poisson's ratio for tank material, dimensionless
ϕ	Thermodynamic function, $\frac{1}{\rho_o} \frac{\partial P}{\partial u}$, psia-ft ³ /btu.
ψ	Line bend angle, degrees.

Subscripts

a	Upstream of a leak
b	Downstream of a leak
B	Source (battery)
c	Cracking
C	Leak leg
g	Gas
i	Inlet
j	Outlet
r	Reseat
R	Residual
s	Sink
T	Total
x	Leak location

Index

I	Gas flag: 1 for hydrogen; 2 for oxygen
J	Tank flag: 1, 2, or 3

APPENDIX II

DERIVATION OF dp/dt FOR VARIABLE VOLUME TANKS DUE TO PRESSURE AND TEMPERATURE CHANGES

Introduction: An expression for the rate of change of pressure for the cryogenic storage tanks has been developed for a constant volume (Reference A-1) and for variable volume caused by tank stretch due to pressure changes (Reference A-2). The latter expression is:

$$\frac{dp}{dt} = \frac{\frac{\phi\theta}{V} \dot{m} + \frac{\phi}{V} q}{1 + \frac{3\phi\phi\rho r}{2tE} (1-\nu)} \quad (1)$$

where:

$$\theta = -\rho \left(\frac{\partial h}{\partial \rho} \right)_p \quad (2)$$

$$\phi = \frac{1}{\rho} \left(\frac{\partial p}{\partial u} \right)_\rho \quad (3)$$

- \dot{m} = Cryogen flowrate, lbm/hr.
- q = Heat flux, BTU/hr.
- V = Volume, cu ft.
- ρ = Density, lbm/cu ft.
- r = Inside tank radius, in.
- t = Wall thickness, in.
- E = Young's Modulus, psi
- ν = Poisson's ratio, dimensionless
- u = Internal energy BTU/lbm
- h = Enthalpy BTU/lbm

If Young's Modulus, E , is taken as infinity (no tank stretch), Equation (1) reduces to the expression for dp/dt as presented in Reference A-1.

The expression for dp/dt considering variable volume resulting from tank stretch due to both pressure and temperature changes is developed in this Appendix. For completeness, a portion of the derivation from Reference A-2 is also presented.

Derivation:

The First Law of Thermodynamics may be written:

$$\frac{dE}{dt} = q + \dot{m} h' - p \frac{dV}{dt}$$

where: E = Energy of the system
 h' = Enthalpy at initial state
 t = Time

If it is assumed that the system is simple at uniform pressure, p , and that kinetic and potential energy may be neglected, then

$$E = mu = \rho Vu$$

and

$$\frac{d(\rho Vu)}{dt} = q + \dot{m} h' - p \frac{dV}{dt}$$

$$u \frac{d(\rho V)}{dt} + \rho V \frac{du}{dt} = q + \dot{m} h' - p \frac{d(mv)}{dt}$$

where: $v = \frac{1}{\rho}$ = specific volume.

Now $u = h - pv$.

Then
$$u \frac{dm}{dt} + \rho V \frac{d(h-pv)}{dt} = q + \dot{m} h' - p \frac{dmv}{dt} - pv \frac{dm}{dt}$$

$$um + \rho V \frac{dh}{dt} - \rho V \frac{d(pv)}{dt} = q + \dot{m} h' - pm \frac{dv}{dt} - p v \dot{m}$$

$$\dot{m}(u + pv) + \rho V \frac{dh}{dt} - \rho V p \frac{dv}{dt} - \rho V v \frac{dp}{dt} = q + \dot{m} h' - pm \frac{dv}{dt}$$

$$\dot{m} h + \rho V \frac{dh}{dt} - m p \frac{dv}{dt} - V \frac{dp}{dt} = q + \dot{m} h' - p m \frac{dv}{dt}$$

$$V \frac{dp}{dt} = \rho V \frac{dh}{dt} - q + \dot{m} (h - h')$$

$$\frac{dp}{dt} = \rho \frac{dh}{dt} - \frac{q}{V} + \frac{\dot{m}}{V} (h - h').$$

Since $h \approx h'$, the last term is negligible.

$$\text{Thus, } \frac{dp}{dt} = \rho \frac{dh}{dt} - \frac{q}{V} \quad (4)$$

Assume that

$$h = h(p, \rho).$$

then

$$\begin{aligned} dh &= \left. \frac{\partial h}{\partial p} \right|_{\rho} dp + \left. \frac{\partial h}{\partial \rho} \right|_p d\rho \\ \frac{dh}{dt} &= \left. \frac{\partial h}{\partial p} \right|_{\rho} \frac{dp}{dt} + \left. \frac{\partial h}{\partial \rho} \right|_p \frac{d\rho}{dt} . \end{aligned}$$

Now,

$$V = \frac{m}{\rho}$$

$$\text{and } \frac{d\rho}{dt} = \frac{d(\frac{m}{V})}{dt} = \frac{1}{V} \frac{dm}{dt} - \frac{m}{V^2} \frac{dV}{dt} = \frac{\rho}{m} \frac{dm}{dt} - \frac{\rho}{V} \frac{dV}{dt} .$$

$$\text{So, } \frac{dh}{dt} = \left. \frac{\partial h}{\partial p} \right|_{\rho} \frac{dp}{dt} + \left. \frac{\partial h}{\partial \rho} \right|_p \left[\frac{\rho}{m} \frac{dm}{dt} - \frac{\rho}{V} \frac{dV}{dt} \right] .$$

Substituting for Θ from Equation (2)

$$\frac{dh}{dt} = \left. \frac{\partial h}{\partial p} \right|_{\rho} \frac{dp}{dt} - \frac{\Theta}{m} \dot{m} + \frac{\Theta}{V} \frac{dV}{dt}$$

$$\text{Since } h = u + pv = u + \frac{p}{\rho} ,$$

$$\text{then } \left. \frac{\partial h}{\partial p} \right|_{\rho} = \left. \frac{\partial u}{\partial p} \right|_{\rho} + \left. \frac{\partial (\frac{p}{\rho})}{\partial p} \right|_{\rho}$$

$$\left. \frac{\partial h}{\partial p} \right|_{\rho} = \left. \frac{\partial u}{\partial p} \right|_{\rho} + \frac{1}{\rho}$$

So,

$$\frac{dh}{dt} = \left[\left. \frac{\partial u}{\partial p} \right|_{\rho} + \frac{1}{\rho} \right] \frac{dp}{dt} - \frac{\Theta}{m} \dot{m} + \frac{\Theta}{V} \frac{dV}{dt} .$$

Substituting for ϕ from Equation (3)

$$\frac{dh}{dt} = \left[\frac{1}{\rho \phi} + \frac{1}{\rho} \right] \frac{dp}{dt} - \frac{\Theta}{m} \dot{m} + \frac{\Theta}{V} \frac{dV}{dt} . \quad (5)$$

It is at this point that the assumption that tank stretch is a function of both pressure, p , and temperature, T .

$$\frac{dV}{dt} = \left. \frac{\partial V}{\partial p} \right|_T \frac{dp}{dt} + \left. \frac{\partial V}{\partial T} \right|_p \frac{dT}{dt} \quad (6)$$

It is necessary to determine dT/dt

$$\frac{dT}{dt} = \left. \frac{\partial T}{\partial p} \right|_\rho \frac{dp}{dt} + \left. \frac{\partial T}{\partial \rho} \right|_p \frac{d\rho}{dt} \quad (7)$$

Now, $m = \rho V$

$$\frac{dm}{dt} = \frac{d\rho}{dt} V + \rho \frac{dV}{dt}$$

$$\text{So,} \quad \frac{d\rho}{dt} = \frac{\dot{m}}{V} - \frac{\rho}{V} \frac{dV}{dt} \quad (8)$$

Substituting Equations (8) into Equation (7), and substituting Equation (7) into Equation (6), results in:

$$\frac{dV}{dt} = \left. \frac{\partial V}{\partial p} \right|_T \frac{dp}{dt} + \left. \frac{\partial V}{\partial T} \right|_p \left[\left. \frac{\partial T}{\partial p} \right|_\rho \frac{dp}{dt} + \left. \frac{\partial T}{\partial \rho} \right|_p \left(\frac{\dot{m}}{V} - \frac{\rho}{V} \frac{dV}{dt} \right) \right]$$

For convenience, the following substitutions have been made:

$$A = \left. \frac{\partial V}{\partial p} \right|_T \quad B = \left. \frac{\partial V}{\partial T} \right|_p$$

$$C = \left. \frac{\partial T}{\partial p} \right|_\rho \quad D = \left. \frac{\partial T}{\partial \rho} \right|_p$$

Then,

$$\frac{dV}{dt} = A \frac{dp}{dt} + B \left[C \frac{dp}{dt} + D \left(\frac{\dot{m}}{V} - \frac{\rho}{V} \frac{dV}{dt} \right) \right]$$

$$\frac{dV}{dt} = (A + BC) \frac{dp}{dt} + BD \frac{\dot{m}}{V} - \frac{BD\rho}{V} \frac{dV}{dt}$$

$$\left(1 + \frac{BD\rho}{V} \right) \frac{dV}{dt} = (A + BC) \frac{dp}{dt} + \frac{BD\dot{m}}{V}$$

$$\frac{dV}{dt} = \frac{(A + BC) \frac{dp}{dt} + \frac{BD\dot{m}}{V}}{1 + \frac{BD\rho}{V}} \quad (9)$$

Substituting Equation (9) into Equation (5),

$$\frac{dh}{dt} = \left[\frac{1}{\rho\phi} + \frac{1}{\rho} \right] \frac{dp}{dt} - \frac{\Theta}{m} \dot{m} + \frac{\Theta}{V} \left[\frac{(A + BC) \frac{dp}{dt} + BD \frac{\dot{m}}{V}}{1 + \frac{BD\rho}{V}} \right]$$

$$\frac{dh}{dt} = \left[\frac{1}{\rho\phi} + \frac{1}{\rho} \right] \frac{dp}{dt} - \frac{\Theta}{m} \dot{m} + \frac{\Theta}{(V+BD\rho)} \left[(A + BC) \frac{dp}{dt} + BD \frac{\dot{m}}{V} \right]$$

$$\frac{dh}{dt} = \left[\frac{1}{\rho\phi} + \frac{1}{\rho} + \frac{\Theta(A + BC)}{V+BD\rho} \right] \frac{dp}{dt} - \frac{\Theta\dot{m}}{m} + \frac{\Theta BD\dot{m}}{V(V+BD\rho)} .$$

But from Equation (4)

$$\frac{dh}{dt} = \frac{1}{\rho} \frac{dp}{dt} + \frac{q}{\rho V} .$$

Therefore,

$$\frac{1}{\rho} \frac{dp}{dt} + \frac{q}{\rho V} = \left[\frac{1}{\rho\phi} + \frac{1}{\rho} + \frac{\Theta(A+BC)}{V+BD\rho} \right] \frac{dp}{dt} - \frac{\Theta\dot{m}}{m} + \frac{\Theta BD\dot{m}}{V(V+BD\rho)}$$

and,

$$\left[\frac{1}{\rho\phi} + \frac{\Theta(A+BC)}{V+BD\rho} \right] \frac{dp}{dt} = \frac{\Theta\dot{m}}{m} - \frac{\Theta BD\dot{m}}{V(V+BD\rho)} + \frac{q}{\rho V}$$

resulting in:

$$\frac{dp}{dt} = \frac{\frac{\Theta\dot{m}}{\rho V} + \frac{q}{\rho V} - \frac{\Theta BD\dot{m}}{V(V+BD\rho)}}{\frac{1}{\rho\phi} + \frac{\Theta(A+BC)}{V+BD\rho}}$$

or,

$$\frac{dp}{dt} = \frac{\frac{\Theta\dot{m}\phi}{V} + \frac{\phi q}{V} - \frac{\Theta\phi BD\dot{m}\rho}{V(V+BD\rho)}}{1 + \frac{\phi\Theta\rho(A+BC)}{V+BD\rho}}$$

Substituting for A, B, C and D

$$\frac{dp}{dt} = \frac{\frac{\Theta\dot{m}\phi}{V} + \frac{\phi q}{V} - \frac{\Theta\phi\dot{m}\rho \left(\frac{\partial V}{\partial T} \Big|_p \frac{\partial T}{\partial \rho} \Big|_p \right)}{V(V+\rho \left(\frac{\partial V}{\partial T} \Big|_p \frac{\partial T}{\partial \rho} \Big|_p \right))}}{1 + \frac{\phi\Theta\rho \left(\frac{\partial V}{\partial p} \Big|_T + \frac{\partial V}{\partial T} \Big|_p \frac{\partial T}{\partial p} \Big|_p \right)}{V + \rho \left(\frac{\partial V}{\partial T} \Big|_p \frac{\partial T}{\partial \rho} \Big|_p \right)}} . \quad (10)$$

Reference A-2 presents the derivation for change in volume with respect to pressure at constant temperature as:

$$\left. \frac{\partial V}{\partial p} \right|_T = \frac{3rV}{2tE} (1-\nu) \quad (11)$$

The change in volume with respect to temperature may be obtained as follows:

$$\begin{aligned} \left. \frac{\partial V}{\partial T} \right|_p &= \left. \frac{\partial V}{\partial r} \right|_p \left. \frac{\partial r}{\partial T} \right|_p \\ \frac{\partial V}{\partial r} &= \frac{\partial}{\partial r} \left(\frac{4}{3} \pi r^3 \right) = 4 \pi r^2 = \frac{3V}{r} \end{aligned}$$

For small changes in temperature, then

$$\left. \frac{\partial V}{\partial T} \right|_p = \frac{3V}{r} \frac{\Delta r}{\Delta T} = 3\alpha V \quad (12)$$

where α = coefficient of thermal expansion, /°R.

Substituting these expressions into Equation (10) results in:

$$\frac{dp}{dt} = \frac{\frac{\phi m \dot{\phi}}{V} + \frac{\phi q}{V} - \frac{\phi \dot{\phi} m 3\alpha \rho \left. \frac{\partial T}{\partial \rho} \right|_p}{V (1 + \rho 3\alpha \left. \frac{\partial T}{\partial \rho} \right|_p)}}{1 + \phi \left(\frac{3r}{2tE} (1-\nu) + 3\alpha \left. \frac{\partial T}{\partial p} \right|_p \right)} \quad (13)$$

$$1 + 3\alpha \rho \left. \frac{\partial T}{\partial \rho} \right|_p$$

It is necessary to account for one additional effect which results in a variation in the change in volume with respect to pressure. This effect is the compression of the fluid in the fill and vent lines of the tank. These lines extend from the pressure vessel to the warm environment. The fluid at the cold ends is relatively incompressible as compared to the near ideal gas conditions at the other ends. When pressure increases, the fluid in the lines is compressed by the expanding stored fluid which move up the lines. To account for this effect, it was assumed that the lines will be filled with an ideal gas at ambient temperature and that no mixing between the tanked cyrogen and the perfect gas would take place. Then:

$$p V_2^n = \text{constant.}$$

where: V_2 = line volume, ft³

n = polytropic exponent equal to 1 for a isothermal process
or the ratio of specific heats for an isentropic process.

Thus,

$$V_2^n \frac{dp}{dt} + npV_2^{n-1} \frac{dV_2}{dt} = 0$$

or

$$\frac{dV_2}{dt} = \frac{-V_2}{np} \frac{dp}{dt} \quad (14)$$

The mass flow, \dot{m} , is the total flow from the tank:

$$\dot{m} = \dot{m}_o + \dot{m}_2 \quad (15)$$

where: \dot{m}_o = flow to EPS and ECS subsystems, lbm/hr

$\dot{m}_2 = \rho \frac{dV_2}{dt}$ = flow from fill and vent lines, lbm/hr

Note: Flow out of the tank is negative in sign.

Substituting Equation (14) into Equation (15) yield:

$$\dot{m} = \dot{m}_o - \rho \frac{V_2}{np} \frac{dp}{dt}$$

When this equation is substituted into equation (13) and rearranged, the resulting expression is:

$$\frac{dp}{dt} = \frac{\frac{\Theta\phi}{V} \dot{m}_o + \frac{\phi}{V} q - \frac{\Theta\phi}{V} \frac{\dot{m}_o}{(1 + \rho \frac{3\alpha}{\partial T} \big|_p)} \frac{3\alpha \frac{\partial T}{\partial \rho} \big|_p}{1 + \frac{\Theta\phi}{V} \frac{\rho V_2}{np} - \frac{\Theta\phi}{V} \frac{V_2 3\alpha \rho^2 \frac{\partial T}{\partial \rho} \big|_p}{np (1 + 3\alpha \rho \frac{\partial T}{\partial \rho} \big|_p)} + \frac{\Theta\phi \rho (\frac{3r}{2tE} (1 - \nu) + 3\alpha \frac{\partial T}{\partial p} \big|_\rho)}{1 + 3\alpha \rho \frac{\partial T}{\partial \rho} \big|_p} \quad (16)$$

Thus, Equation (16) describes the rate of change of pressure for a variable tank volume considering both pressure and temperature changes. Note that if the coefficient of thermal expansion, α , is equal to zero and if the plumbing fluid compression volume, V_2 , is zero that Equation (1) is obtained. Table A-1 presents the constants used for both the oxygen and hydrogen tanks. The partial derivatives are obtained by differentiating the equation of state. Since the EQTANK program uses an equation of state that is a function of temperature and density, it is desirable to obtain $\partial T / \partial \rho$ in the following form:

$$\frac{\partial T}{\partial \rho} \big|_p \frac{\partial \rho}{\partial p} \big|_T \frac{\partial p}{\partial T} \big|_\rho = -1$$

This relation was taken from Reference A-4, page 32, Equation (3-11).

Then

$$\left. \frac{\partial T}{\partial \rho} \right|_p = - \frac{1}{\left. \frac{\partial \rho}{\partial p} \right|_T \left. \frac{\partial p}{\partial T} \right|_\rho} = - \left. \frac{\partial p}{\partial \rho} \right|_T \left. \frac{\partial T}{\partial p} \right|_\rho$$

Thus, this partial derivative may also be obtained from the equation of state.

TABLE A-1

CRYOGENIC TANK PROPERTIES

OXYGEN

Material.....	Inconel 718
Volume, V , ft^3	4.75
Inside Radius, r , in.....	12.513
Young's Modulus, E , psi.....	30×10^6
Poisson's Ratio, ν , dimensionless.....	0.29
Wall Thickness, t , in.....	0.059
Coefficient of Thermal Expansion, α , $/^\circ\text{R}$	5.93×10^{-6}

HYDROGEN

Material.....	Titanium-5AL-2.5SN ELI
Volume, V , ft^3	6.80
Inside Radius, r , in.....	14.103
Young's Modulus, E , psi.....	17×10^6
Poisson's Ratio, ν , dimensionless.....	0.30
Wall Thickness, t , in.....	0.044
Coefficient of Thermal Expansion, α , $/^\circ\text{R}$	1.23×10^{-6}

Note: Values for α were derived from Reference A-3, Table 7.3.4, page 7-59.

APPENDIX II REFERENCES

- A-1. TRW IOC 70.4354.3-84, "Thermodynamics Relations for the Quasi-Static Flow of Single Phase Fluids," C. E. Barton, 17 August 1970.
- A-2. TRW IOC 70.4352.36-2, "Derivation of the Cryogenic Pressure Rise/Decay Rates," C. W. Wurst, 26 October 1970.
- A-3. "Apollo Fuel Cell and Cryogenic Gas Storage System Flight Support Handbook," NASA/MSC, 18 February 1970.
- A-4. Thermodynamics, the Kinetic Theory of Gases, and Statistical Mechanics, F. W. Sears, Addison-Wesley Publishing, 1953.

APPENDIX III

COMPONENT AND LINE MATRIX MODEL EQUATIONS

Oxygen System Equations

The lumped parameter equations for the oxygen system matrix model are given below. The equations are shown for each node as a function of the failure mode. Node locations are shown in Figure A-1.

A. Node 1

1) No leaks

$$G_2 (E_{B1} - E_1) = C_1 \frac{dE_1}{dt} + G_1 E_1 + G_3 (E_1 - E_2) - I_{R1}$$

2) Leak in Leg 2

$$G_{2b} (E_{2x} - E_1) = C_1 \frac{dE_1}{dt} + G_1 E_1 + G_3 (E_1 - E_2) - I_{R1}$$

3) Leak in Leg 3

$$G_2 (E_{B1} - E_1) = C_1 \frac{dE_1}{dt} + G_1 E_1 + G_{3a} (E_1 - E_{3x}) - I_{R1}$$

4) Leak in Leg 2 and 3

$$G_{2b} (E_{2x} - E_1) = C_1 \frac{dE_1}{dt} + G_1 E_1 + G_{3a} (E_1 - E_{3x}) - I_{R1}$$

B. Node 2

1) No leaks

$$G_3 (E_1 - E_2) = C_2 \frac{dE_2}{dt} + G_4 (E_2 - E_4) + G_{10} (E_2 - E_{10}) - I_{R2}$$

2) Leak in Leg 3

$$G_{3b} (E_{3x} - E_2) = C_2 \frac{dE_2}{dt} + G_4 (E_2 - E_4) + G_{10} (E_2 - E_{10}) - I_{R2}$$

3) Leak in Leg 4

$$G_3 (E_1 - E_2) = C_2 \frac{dE_2}{dt} + G_{4a} (E_2 - E_{4x}) + G_{10} (E_2 - E_{10}) - I_{R2}$$

4) Leak in Leg 10

$$G_3 (E_1 - E_2) = C_2 \frac{dE_2}{dt} + G_4 (E_2 - E_4) + G_{10a} (E_2 - E_{10x}) - I_{R2}$$

5) Leak in Leg 3 and Leg 4

$$G_{3b} (E_{3x} - E_2) = C_2 \frac{dE_2}{dt} + G_{4a} (E_2 - E_{4x}) + G_{10} (E_2 - E_{10}) - I_{R2}$$

6) Leak in Leg 3 and Leg 10

$$G_{3b} (E_{3x} - E_2) = C_2 \frac{dE_2}{dt} + G_4 (E_2 - E_4) + G_{10a} (E_2 - E_{10x}) - I_{R2}$$

7) Leak in Leg 4 and Leg 10

$$G_3 (E_1 - E_2) = C_2 \frac{dE_2}{dt} + G_{4a} (E_2 - E_{4x}) + G_{10a} (E_2 - E_{10x}) - I_{R2}$$

C. Node 3

1) No leaks

$$G_7 (E_{B2} - E_3) = C_3 \frac{dE_3}{dt} + G_6 (E_3 - E_5) + G_5 (E_3 - E_4) - I_{R3}$$

2) Leak in Leg 7

$$G_{7b} (E_{7x} - E_3) = C_3 \frac{dE_3}{dt} + G_6 (E_3 - E_5) + G_5 (E_3 - E_4) - I_{R3}$$

3) Leak in Leg 6

$$G_7 (E_{B2} - E_3) = C_3 \frac{dE_3}{dt} + G_{6a} (E_3 - E_{6x}) + G_5 (E_3 - E_4) - I_{R3}$$

4) Leak in Leg 5

$$G_7(E_{B2} - E_3) = C_3 \frac{dE_3}{dt} + G_6(E_3 - E_5) + G_{5a}(E_3 - E_{5x}) - I_{R3}$$

5) Leak in Leg 7 and Leg 8

$$G_{7b}(E_{7x} - E_3) = C_3 \frac{dE_3}{dt} + G_{6a}(E_3 - E_{6x}) + G_5(E_3 - E_4) - I_{R3}$$

6) Leak in Leg 7 and Leg 5

$$G_{7b}(E_{7x} - E_3) = C_3 \frac{dE_3}{dt} + G_6(E_3 - E_5) + G_{5a}(E_3 - E_{5x}) - I_{R3}$$

7) Leak in Leg 6 and Leg 5

$$G_7(E_{B2} - E_3) = C_3 \frac{dE_3}{dt} + G_{6a}(E_3 - E_{6x}) + G_{5a}(E_3 - E_{5x}) - I_{R3}$$

D. Node 4

1) No Leaks

$$G_5(E_3 - E_4) + G_4(E_2 - E_4) = C_4 \frac{dE_4}{dt} + G_8(E_4 - E_6) - I_{R4}$$

2) Leak in Leg 5

$$G_{5b}(E_{5x} - E_4) + G_4(E_2 - E_4) = C_4 \frac{dE_4}{dt} + G_8(E_4 - E_6) - I_{R4}$$

3) Leak in Leg 4

$$G_5(E_3 - E_4) + G_{4b}(E_{4x} - E_4) = C_4 \frac{dE_4}{dt} + G_8(E_4 - E_6) - I_{R4}$$

4) Leak in Leg 8

$$G_5(E_3 - E_4) + G_4(E_{4x} - E_4) = C_4 \frac{dE_4}{dt} + G_{8a}(E_4 - E_{8x}) - I_{R4}$$

5) Leak in Leg 5 and Leg 4

$$G_{5b}(E_{5x} - E_4) + G_{4b}(E_{4x} - E_4) = C_4 \frac{dE_4}{dt} + G_8(E_4 - E_6) - I_{R4}$$

6) Leak in Leg 5 and Leg 8

$$G_{5b}(E_{5x} - E_4) + G_4(E_2 - E_4) = C_4 \frac{dE_4}{dt} + G_{8a}(E_4 - E_{8x}) - I_{R4}$$

7) Leak in Leg 4 and Leg 8

$$G_5(E_3 - E_4) + G_{4b}(E_{4x} - E_4) = C_4 \frac{dE_4}{dt} + G_{8a}(E_4 - E_{8x}) - I_{R4}$$

E. Node 5

1) No leaks

$$G_6(E_3 - E_5) + G_{13}(E_7 - E_5) = C_5 \frac{dE_5}{dt} + G_{15} E_5 - I_{R5}$$

2) Leak in Leg 6

$$G_{6b}(E_{6x} - E_5) + G_{13}(E_7 - E_5) = C_5 \frac{dE_5}{dt} + G_{15} E_5 - I_{R5}$$

3) Leak in Leg 13

$$G_6(E_3 - E_5) + G_{13b}(E_{13x} - E_5) = C_5 \frac{dE_5}{dt} + G_{15} E_5 - I_{R5}$$

4) Leak in Leg 6 and Leg 13

$$G_{6b}(E_{6x} - E_5) + G_{13b}(E_{13x} - E_5) = C_5 \frac{dE_5}{dt} + G_{15} E_5 - I_{R5}$$

F. Node 6

1) No leaks

$$G_8(E_4 - E_6) + G_9(E_8 - E_6) = I_1 + C_6 \frac{dE_6}{dt} - I_{R6}$$

2) Leak in Leg 8

$$G_{4b}(E_{4x} - E_6) + G_9(E_8 - E_6) = I_1 + C_6 \frac{dE_6}{dt} - I_{R6}$$

3) Leak in Leg 9

$$G_8(E_4 - E_6) + G_{9a}(E_{9x} - E_6) = I_1 + C_6 \frac{dE_6}{dt} - I_{R6}$$

4) Leak in Leg 8 and Leg 9

$$G_{4b}(E_{4x} - E_6) + G_{9a}(E_{9x} - E_6) = I_1 + C_6 \frac{dE_6}{dt} - I_{R6}$$

G. Node 7

1) No leaks

$$G_{11}(E_{B3} - E_7) = C_7 \frac{dE_7}{dt} + G_{13}(E_7 - E_5) + G_{12}(E_7 - E_8) - I_{R7}$$

2) Leak in Leg 11

$$G_{11b}(E_{11x}-E_7) = C_7 \frac{dE_7}{dt} + G_{13}(E_7-E_5) + G_{12}(E_7-E_8) - I_{R7}$$

3) Leak in Leg 12

$$G_{11}(E_{B3}-E_7) = C_7 \frac{dE_7}{dt} + G_{13}(E_7-E_5) + G_{12a}(E_7-E_{12x}) - I_{R7}$$

4) Leak in Leg 13

$$G_{11}(E_{B3}-E_7) = C_7 \frac{dE_7}{dt} + G_{13a}(E_7-E_{13x}) + G_{12}(E_7-E_8) - I_{R7}$$

5) Leak in Leg 11 and Leg 12

$$G_{11b}(E_{11x}-E_7) = C_7 \frac{dE_7}{dt} + G_{13}(E_7-E_5) + G_{12a}(E_7-E_{12x}) - I_{R7}$$

6) Leak in Leg 11 and Leg 13

$$G_{11b}(E_{11x}-E_7) = C_7 \frac{dE_7}{dt} + G_{13a}(E_7-E_{13x}) + G_{12}(E_7-E_8) - I_{R7}$$

7) Leak in Leg 12 and Leg 13

$$G_{11}(E_{B3}-E_7) = C_7 \frac{dE_7}{dt} + G_{13a}(E_7-E_{13x}) + G_{12a}(E_7-E_{12}) - I_{R7}$$

H. Node 8

1) No Leaks

$$G_{12}(E_7-E_8) = C_8 \frac{dE_8}{dt} + G_9(E_8-E_6) + G_{14}(E_8-E_{11}) - I_{R8}$$

2) Leak in Leg 12

$$G_{12b}(E_{12x}-E_8) = C_8 \frac{dE_8}{dt} + G_9(E_8-E_6) + G_{14}(E_8-E_{11}) - I_{R8}$$

3) Leak in Leg 9

$$G_{12}(E_7-E_8) = C_8 \frac{dE_8}{dt} + G_{9a}(E_8-E_{9x}) + G_{14}(E_8-E_{11}) - I_{R8}$$

4) Leak in Leg 14

$$G_{12}(E_7-E_8) = C_8 \frac{dE_8}{dt} + G_9(E_8-E_6) + G_{14a}(E_8-E_{14x}) - I_{R8}$$

5) Leak in Leg 12 and Leg 9

$$G_{12b}(E_{12x}-E_8) = C_8 \frac{dE_8}{dt} + G_{9a}(E_8-E_{9x}) + G_{14}(E_8-E_{11}) - I_{R8}$$

6) Leak in Leg 12 and Leg 14

$$G_{12b}(E_{12x} - E_8) = C_8 \frac{dE_8}{dt} + G_9(E_8 - E_6) + G_{14a}(E_8 - E_{14}) - I_{R8}$$

7) Leak in Leg 9 and Leg 14

$$G_{12}(E_7 - E_8) = C_8 \frac{dE_8}{dt} + G_{9a}(E_8 - E_{9x}) + G_{14a}(E_8 - E_{14}) - I_{R8}$$

I. Node 9

1) No leaks

$$G_{17}(E_{11} - E_9) + G_{16}(E_{10} - E_9) = C_9 \frac{dE_9}{dt} + I_2 - I_{R9}$$

2) Leak in Leg 17

$$G_{17b}(E_{17x} - E_9) + G_{16}(E_{10} - E_9) = C_9 \frac{dE_9}{dt} + I_2 - I_{R9}$$

3) Leak in Leg 16

$$G_{17}(E_{11} - E_9) + G_{16b}(E_{16x} - E_9) = C_9 \frac{dE_9}{dt} = I_2 - I_{R9}$$

4) Leak in Leg 16 and Leg 17

$$G_{17b}(E_{17x} - E_9) + G_{16b}(E_{16x} - E_9) = C_9 \frac{dE_9}{dt} = I_2 - I_{R9}$$

J. Node 10

1) No leaks

$$G_{10}(E_2 - E_{10}) = C_{10} \frac{dE_{10}}{dt} + G_{16}(E_{10} - E_9) - I_{R10}$$

2) Leak in Leg 10

$$G_{10b}(E_{10x} - E_{10}) = C_{10} \frac{dE_{10}}{dt} + G_{16}(E_{10} - E_9) - I_{R10}$$

3) Leak in Leg 16

$$G_{10}(E_2 - E_{10}) = C_{10} \frac{dE_{10}}{dt} + G_{16a}(E_{10} - E_{16x}) - I_{R10}$$

4) Leak in Leg 10 and Leg 16

$$G_{10b}(E_{10x} - E_{10}) = C_{10} \frac{dE_{10}}{dt} + G_{16a}(E_{10} - E_{16x}) - I_{R10}$$

K. Node 11

1) No leaks

$$G_{14}(E_8 - E_{11}) = C_{11} \frac{dE_{11}}{dt} + G_{17}(E_{11} - E_9) - I_{R11}$$

2) Leak in Leg 14

$$G_{14b}(E_{14x} - E_{11}) = C_{11} \frac{dE_{11}}{dt} + G_{17}(E_{11} - E_9) - I_{R11}$$

3) Leak in Leg 17

$$G_{14}(E_8 - E_{11}) = C_{11} \frac{dE_{11}}{dt} + G_{17a}(E_{11} - E_{17x}) - I_{R11}$$

4) Leak in Leg 14 and Leg 17

$$G_{14b}(E_{14x} - E_{11}) = C_{11} \frac{dE_{11}}{dt} + G_{17a}(E_{11} - E_{17x}) - I_{R11}$$

L. Node X

1) Leak in Leg 2

$$G_{2a}(E_{B1} - E_{2x}) = G_{2b}(E_{2x} - E_1) + G_{2C} E_{2x}$$

2) Leak in Leg 3

$$G_{3a}(E_1 - E_{3x}) = G_{3b}(E_{3x} - E_2) + G_{3C} E_{3x}$$

3) Leak in Leg 4

$$G_{4a}(E_2 - E_{4x}) = G_{4b}(E_{4x} - E_4) + G_{4C} E_{4x}$$

4) Leak in Leg 5

$$G_{5a}(E_3 - E_{5x}) = G_{5b}(E_{5x} - E_4) + G_{5C} E_{5x}$$

5) Leak in Leg 6

$$G_{6a}(E_3 - E_{6x}) = G_{6b}(E_{6x} - E_5) + G_{6C} E_{6y}$$

6) Leak in Leg 7

$$G_{7a}(E_{B2} - E_{7x}) = G_{7b}(E_{7x} - E_3) + G_{7C} E_{7x}$$

7) Leak in Leg 8

$$G_{8a}(E_4 - E_{7x}) = G_{8b}(E_{8x} - E_6) + G_{8c} E_{7x}$$

8) Leak in Leg 9

$$G_{9a}(E_8 - E_{9x}) = G_{9b}(E_{9x} - E_6) + G_{9c} E_{9x}$$

9) Leak in Leg 10

$$G_{10a}(E_7 - E_{10x}) = G_{10b}(E_{10x} - E_{11}) + G_{10c} E_{10x}$$

10) Leak in Leg 11

$$G_{11a}(E_{B3} - E_{11x}) = G_{11b}(E_{11x} - E_7) + G_{11c} E_{11x}$$

11) Leak in Leg 12

$$G_{12a}(E_7 - E_{12x}) + G_{12b}(E_{12x} - E_8) + G_{12c} E_{12x}$$

12) Leak in Leg 13

$$G_{13a}(E_7 - E_{13x}) = G_{13b}(E_{B_x} - E_5) + G_{13c} E_{13x}$$

13) Leak in Leg 14

$$G_{14a}(E_8 - E_{14x}) = G_{14b}(E_{14x} - E_{12}) + G_{14c} E_{14x}$$

14) Leak in Leg 16

$$G_{16a}(E_{10} - E_{16x}) = G_{16b}(E_{16x} - E_9) + G_{16c} E_{16x}$$

15) Leak in Leg 17

$$G_{17a}(E_{11} - E_{17x}) = G_{17b}(E_{17x} - E_9) + G_{17c} E_{17x}$$

Hydrogen System Equations

The equations for the hydrogen system are given below. These equations are presented for each node as a function of failure mode. Node locations are shown in Figure A-2.

A. Node 1

1) No Leaks

$$G_1(E_{B1}-E_1) = G_4(E_1-E_2) + G_7(E_1-E_5) + C_1 \frac{dE_1}{dt} - I_{R1}$$

2) Leak in Leg 1

$$G_{1b}(E_{1x}-E_1) = G_4(E_1-E_2) + G_7(E_1-E_5) + C_1 \frac{dE_1}{dt} - I_{R1}$$

3) Leak in Leg 4

$$G_1(E_{B1}-E_1) = G_{4a}(E_1-E_{4x}) + G_7(E_1-E_5) + C_1 \frac{dE_1}{dt} - I_{R1}$$

4) Leak in Leg 7

$$G_1(E_{B1}-E_1) = G_4(E_1-E_2) + G_{7a}(E_1-E_{7x}) + C_1 \frac{dE_1}{dt} - I_{R1}$$

5) Leak in Leg 1 and Leg 4

$$G_{1b}(E_{1x}-E_1) = G_{4a}(E_1-E_{4x}) + G_7(E_1-E_5) + C_1 \frac{dE_1}{dt} - I_{R1}$$

6) Leak in Leg 1 and Leg 7

$$G_{1b}(E_{1x}-E_1) = G_4(E_1-E_2) + G_{7a}(E_1-E_{7x}) + C_1 \frac{dE_1}{dt} - I_{R1}$$

7) Leak in Leg 4 and Leg 7

$$G_1(E_{B1}-E_1) = G_{4a}(E_1-E_{4x}) + G_{7a}(E_1-E_{7x}) + C_1 \frac{dE_1}{dt} - I_{R1}$$

B. Node 2

1) No Leaks

$$G_4(E_1-E_2) + G_5(E_3-E_2) = G_2 E_2 + \frac{C_2}{dt} \frac{d(E_2)}{dt} - I_{R2}$$

2) Leak in Leg 4

$$G_{4b}(E_{4x}-E_2) + G_5(E_3-E_2) = G_2 E_2 + C_2 \frac{dE_2}{dt} - I_{R2}$$

3) Leak in Leg 5

$$G_4(E_1-E_2) + G_{5b}(E_{5x}-E_2) = G_2 E_2 + C_2 \frac{dE_2}{dt} - I_{R2}$$

4) Leak in Leg 4 and Leg 5

$$G_{4b}(E_{4x}-E_2) + G_{5b}(E_{5x}-E_2) = G_2 E_2 + C_2 \frac{dE_2}{dt} - I_{R2}$$

C. Node 3

1) No Leaks

$$G_3(E_{B2}-E_3) = G_5(E_3-E_2) + G_6(E_3-E_4) + C_3 \frac{dE_3}{dt} - I_{R3}$$

2) Leaks in Leg 3

$$G_{3b}(E_{3x}-E_3) = G_5(E_3-E_2) + G_6(E_3-E_4) + C_3 \frac{dE_3}{dt} - I_{R3}$$

3) Leak in Leg 5

$$G_3(E_{B2}-E_3) = G_{5a}(E_3-E_{5x}) + G_6(E_3-E_4) + C_3 \frac{dE_3}{dt} - I_{R3}$$

4) Leak in Leg 6

$$G_3(E_{B2}-E_3) = G_5(E_3-E_2) + G_{6a}(E_3-E_{6x}) + C_3 \frac{dE_3}{dt} - I_{R3}$$

5) Leak in Leg 3 and Leg 5

$$G_{3b}(E_{3x}-E_3) = G_{5a}(E_3-E_{5x}) + G_6(E_3-E_4) + C_3 \frac{dE_3}{dt} - I_{R3}$$

6) Leak in Leg 3 and Leg 6

$$G_{3b}(E_{3x}-E_3) = G_5(E_3-E_2) + G_{6a}(E_3-E_{6x}) + C_3 \frac{dE_3}{dt} - I_{R3}$$

7) Leak in Leg 5 and Leg 6

$$G_3(E_{B2}-E_3) = G_{5a}(E_3-E_{5x}) + G_{6a}(E_3-E_{6x}) + C_3 \frac{dE_3}{dt} - I_{R3}$$

D. Node 4

1) No Leaks

$$G_6(E_3-E_4) + G_8(E_5-E_4) = C_4 \frac{dE_4}{dt} + I_1 - I_{R4}$$

2) Leak in Leg 6

$$G_{6b}(E_{6x}-E_4) + G_8(E_5-E_4) = C_4 \frac{dE_4}{dt} + I_1 - I_{R4}$$

3) Leak in Leg 8

$$G_6(E_3-E_4) + G_{8b}(E_{8x}-E_4) = C_4 \frac{dE_4}{dt} + I_1 - I_{R4}$$

4) Leak in Leg 6 and Leg 7

$$G_{6b}(E_{6x}-E_4) + G_{8b}(E_{8x}-E_4) = C_4 \frac{dE_4}{dt} + I_1 - I_{R4}$$

E. Node 5

1) No Leaks

$$G_7(E_1 - E_5) = C_5 \frac{dE_5}{dt} + G_8(E_5 - E_4)$$

2) Leak in Leg 7

$$G_{7b}(E_{7x} - E_5) = C_5 \frac{dE_5}{dt} + G_8(E_5 - E_4)$$

3) Leak in Leg 8

$$G_7(E_1 - E_5) = C_5 \frac{dE_5}{dt} + G_{8a}(E_5 - E_{8x})$$

4) Leak in Leg 7 and Leg 8

$$G_{7b}(E_{7x} - E_5) = C_5 \frac{dE_5}{dt} + G_{8a}(E_5 - E_{8x})$$

F. Node X

1) Leak in Leg 1

$$G_{1a}(E_{B1} - E_{1x}) = G_{1b}(E_{1x} - E_1) + G_{1c} E_{1x}$$

2) Leak in Leg 3

$$G_{3a}(E_{B2} - E_{3x}) = G_{3b}(E_{3x} - E_3) + G_{3c} E_{3x}$$

3) Leak in Leg 4

$$G_{4a}(E_1 - E_{4x}) = G_{4b}(E_{1x} - E_2) + G_{4c} E_{4x}$$

4) Leak in Leg 5

$$G_{5a}(E_3 - E_{5x}) = G_{5b}(E_{5x} - E_2) + G_{5c} E_{5x}$$

5) Leak in Leg 6

$$G_{6a}(E_3 - E_{6x}) = G_{6b}(E_{6x} - E_4) + G_{6c} E_{6x}$$

6) Leak in Leg 7

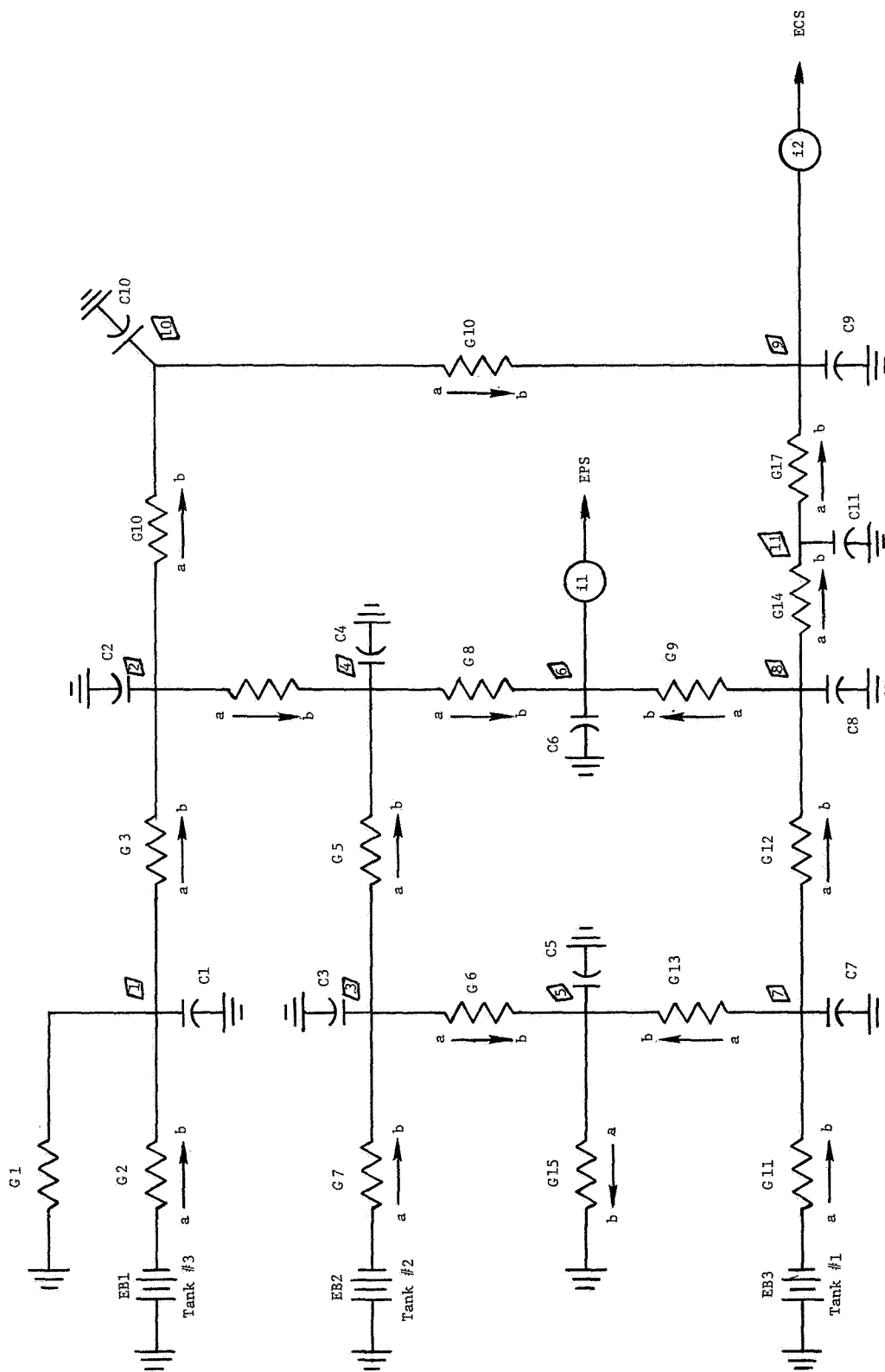
$$G_{7a}(E_1 - E_{7x}) = G_{7b}(E_{7x} - E_4) + G_{7c} E_{7x}$$

7) Leak in Leg 8

$$G_{8a} (E_5 - E_{8x}) = G_{8b} (E_{8x} - E_4) + G_{7c} E_{7x}$$

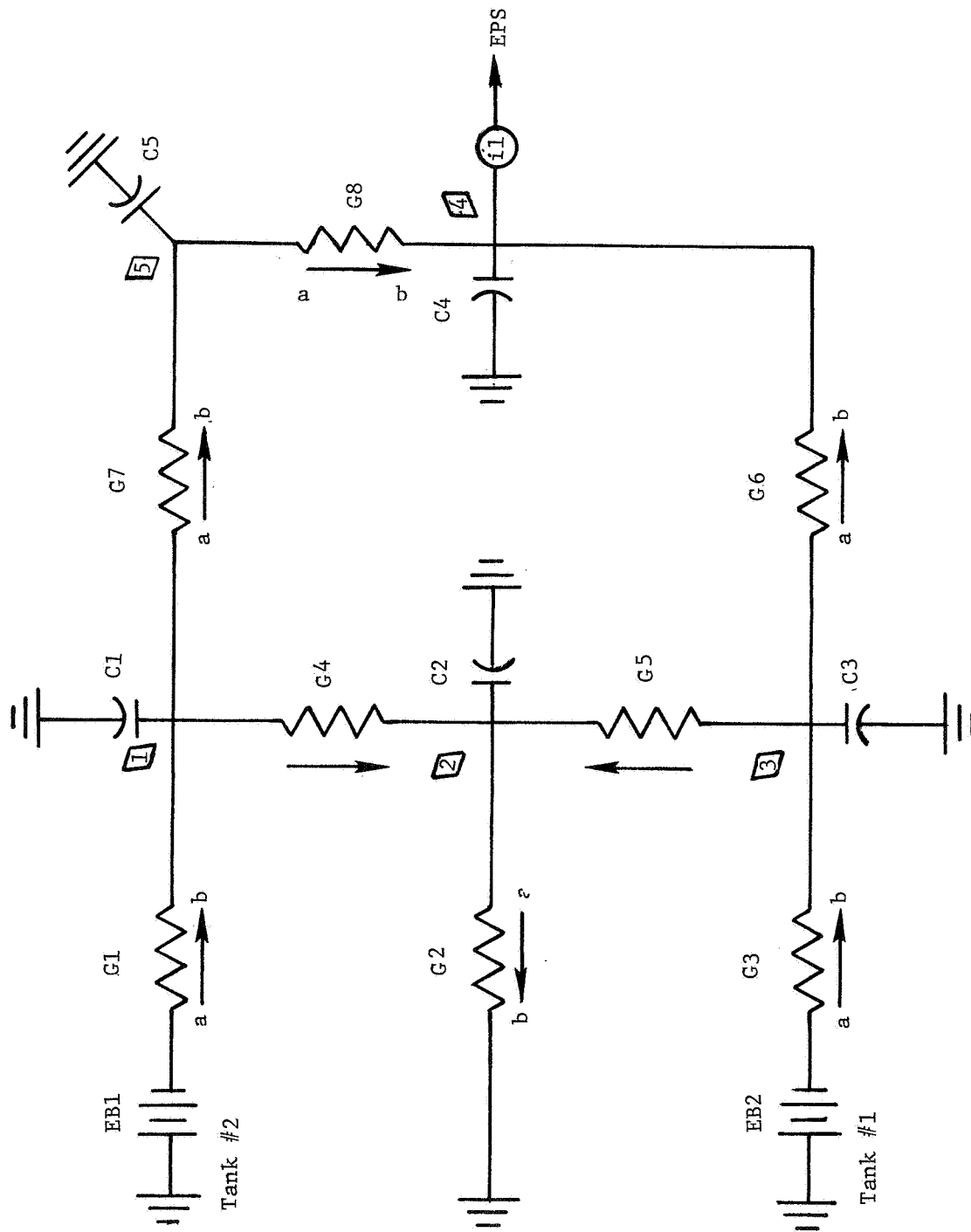
When no leaks are defined in the system, the model is programmed to use the first equation for each lumped parameter node in describing the network. When a leak is defined by a nodal model network node number (not to be confused with a lumped parameter node), the line leg in which that node is located is automatically determined. The two lumped parameter nodes that bound this leg are also determined. The lumped parameter equations for these two nodes are then replaced by the appropriate leak equation presented above. An additional lumped parameter expression is required to solve the new network of equations and is automatically obtained from the Node X equations for the appropriate leg. The relative locations of the lumped parameter nodes and the nodal model network nodes are shown in Figures 3.10 and 3.11 of Section 3.3 for the oxygen and hydrogen systems, respectively. The line legs which correspond to the nodal model network nodes are given in Tables A-2 and A-3 for the oxygen and hydrogen systems, respectively.

Figure A-1
Lumped Parameter Model
H Mission Oxygen System
Lines and Components



a Upstream
b Downstream
Cx Capacitance Analog
EBx Electrical Potential Analog for Tanks
Gx Conductance Analog
ix Flow Demand
ix Lumped Parameter Nodes

Figure A-2
Lumped Parameter Network
H Mission Hydrogen System
Lines and Components



a Upstream
b Downstream
Cx Capacitance Analog
EBx Electrical Potential Analog
for Tanks

Gx Conductance Analog
(ix) Flow Demand
x Lumped Parameter Nodes

Table A-2 - Oxygen System Lumped Parameter Nodal Constants

LUMPED PARAMETER NODE	VOLUME (IN ³)
1	9.12
2	13.66
3	1.9
4	4.28
5	4.98
6	5.0
7	1.9
8	13.32
9	5.18
10	0.93
11	0.08

Table A-3 - Hydrogen System Lumped Parameter Nodal Constants

LUMPED PARAMETER NODE	VOLUME IN ³
1	1.90
2	35.18
3	2.60
4	5.0
5	1.42